Numerical Investigation of Diameter Effect on Heat Transfer of Supercritical Water Flows in Horizontal Round Tubes

Zhi Shang, Shuo Chen

Accepted Manuscript

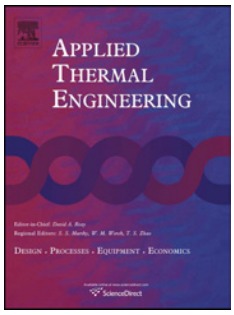

Title: Numerical Investigation of Diameter Effect on Heat Transfer of Supercritical Water Flows in Horizontal Round Tubes

Authors: Zhi Shang, Shuo Chen

PII: S1359-4311(10)00447-3

DOI: 10.1016/j.applthermaleng.2010.10.020

Reference: ATE 3278

To appear in: *Applied Thermal Engineering*

Received Date: 10 June 2010

Revised Date: 25 August 2010

Accepted Date: 15 October 2010

Please cite this article as: Z. Shang, S. Chen. Numerical Investigation of Diameter Effect on Heat Transfer of Supercritical Water Flows in Horizontal Round Tubes, Applied Thermal Engineering (2010), doi: 10.1016/j.applthermaleng.2010.10.020

Numerical Investigation of Diameter Effect on Heat Transfer of Supercritical Water Flows in Horizontal Round Tubes

Zhi Shang[a,b*], Shuo Chen[c]

[a] Science and Technology Facilities Council, Daresbury Laboratory, Warrington WA4 4AD, UK

[b] Faculty of Engineering, Kingston University, London SW15 3DW, UK

[c] School of Aerospace Engineering and Applied Mechanics, Tongji University, Shanghai 200092, China

Abstract

The diameter effect on the heat transfer of supercritical water (SCW) flows in horizontal round tubes has been studied using computational fluid dynamics (CFD) technique. The numerical simulations are carried out by the STAR-CD solver combined with the user developed subroutines that control the numerical calculation procedures. Through the tests it is found that the discretization scheme using CD, LUD or MARS will not affect the accuracy of the numerical simulations. Through the diameter effect studies, it is found that the heat transfer of supercritical water flows in the horizontal round tube is strongly affected by the buoyancy especially for the large diameter tube. The large diameter (D=10mm) tube will have the high risk to have the strong heat transfer deterioration that can introduce 180^{o}C wall temperature difference between the top and bottom surfaces due to the buoyancy effects. The magnitudes of the effects can be quantificationally expressed by a ratio of Grashof number over Reynolds number square. Under the high mass flux regime, the heat transfer deterioration will disappear for all the diameters from 5mm to 10mm. The different secondary flow patterns at different tube diameters are also studied.

Keywords: SCW, CFD, heat transfer, buoyancy, diameter, horizontal tube

Corresponding author. Tel.: +44-19-25603149; Fax: +44-19-25603634
E-mail address: shangzhi@tsinghua.org.cn; zhi.shang@stfc.ac.uk

Nomenclature

Subscripts and index sets

b	bulk temperature
i,j,k	coordinate alternation index
ref	reference value

Parameters

c_p	specific heat capacity, kJ/(kg K) or kJ/(kg ^oC)
$C_{\varepsilon 1-\varepsilon 4}$	turbulent empirical constants
C_μ	empirical coefficient
D	tube diameter, mm
f_μ	damping coefficient
g	gravity acceleration, m/s^2
Gr	Grashof number
h	enthalpy, kJ/kg
k	turbulence kinetic energy, m^2/s^2
l	turbulent eddy scale length, m
L	tube length, m
Nu	Nusselt number
p	pressure, MPa
P_{NL}	non-linear term of turbulence kinetic energy
Pr	Prandtl number
r	radius coordinate, mm
R	tube radius, mm
Re	Reynolds number
Re_l	turbulent eddy scale Reynolds number
s_m	source of momentum equation
s_h	source of energy equation
S_{ij}	mean strain tensor
t	time, s
T	temperature, K or ^oC
u	velocity, m/s
V	velocity magnitude, m/s
x	x coordinate, m
y	y coordinate, m
y^+	non-dimensional distance from wall
α	heat conductivity, W/(K m) or W/(^oC m)
β	fluid thermal expansion, 1/K or 1/^oC
δ	Kronecker delta
ε	dissipation rate of turbulent kinetic energy, m^2/s^3
θ	circumference angle, ^{o}
μ	dynamic viscosity, kg/m s
μ_t	turbulent viscosity, kg/m s
ν	kinetic viscosity, m^2/s
ρ	fluid density, kg/m^3
$\sigma_h,\sigma_k,\sigma_\varepsilon$	Turbulent Prandtl numbers
ϕ	field variable

1. Introduction

The applications about the flow and heat transfer of supercritical water, shorten as SCW, have taken a long time since 1930s. Supercritical water and fluid have many special characters that can be used in many special industrial areas. In the biomass gasification, the supercritical water is employed to generate hydrogen in [1]. Supercritical carbon dioxide is used as the working fluid to produce power and heat by the instrument utilizing solar energy in [2]. In nuclear industry, Atomic Energy of Canada Limited (AECL) has the long-term plan to develop the supercritical water reactor (SCWR) CANDU that is for generation IV nuclear reactor. This kind of nuclear reactor will have the higher thermal efficiency compared with the light water reactor of generation III and generation III+ in [3]. Recently, the more advanced concept of the supercritical water fast reactor has already been put forward in [4-5].

SCW has the gas-like characteristic of low viscosity, and the liquid-like characteristic of high density. Near the pseudo-critical temperature, SCW has the dramatic variations of the physical properties in [6]. Therefore, it is important for users to understand the behaviors of the heat transfer of SCW affected by these characteristics when SCW is employed.

Now some empirical correlations are available for predicting the heat transfer of SCW of [7-8] in the tube. However, almost all the correlations are based on the one-dimensional theoretical analysis without considering the

3D effect. Actually, in the horizontal tube flow, the gravity and buoyancy will affect the flow and heat transfer. Usually, these effects will introduce a full-3D flow in the horizontal tube in [9-10]. Therefore, it is necessary to use a multi dimensional method to analyze the flows in horizontal tubes.

At present, some of CFD codes such as STAR-CD, FLUENT and CFX had been adopted for 3D numerical simulations of supercritical water flows and heat transfers in the vertical channels in [11-13]. In this paper, STAR-CD code is employed to study the flow and heat transfer of SCW in the horizontal tubes. Through the studies, the effects of tube diameters on the flow and heat transfer are investigated.

2. Thermal physical properties of SCW

In this paper, the thermal-physical properties of SCW are taken from the latest releases of the International Association of Properties of Water and Steam (IAPWS). Although there is no liquid-vapor phase transition, the thermal-physical properties of SCW always vary following the temperature changes. The sharp changes of properties exist in the vicinity around the pseudo-critical temperature, shown in Fig. 1. Through the studies in [9, 11-13], it is found that the thermal-physical properties of SCW affect the heat transfer of SCW straightly. Therefore the various thermal physical properties have to be considered during CFD simulations.

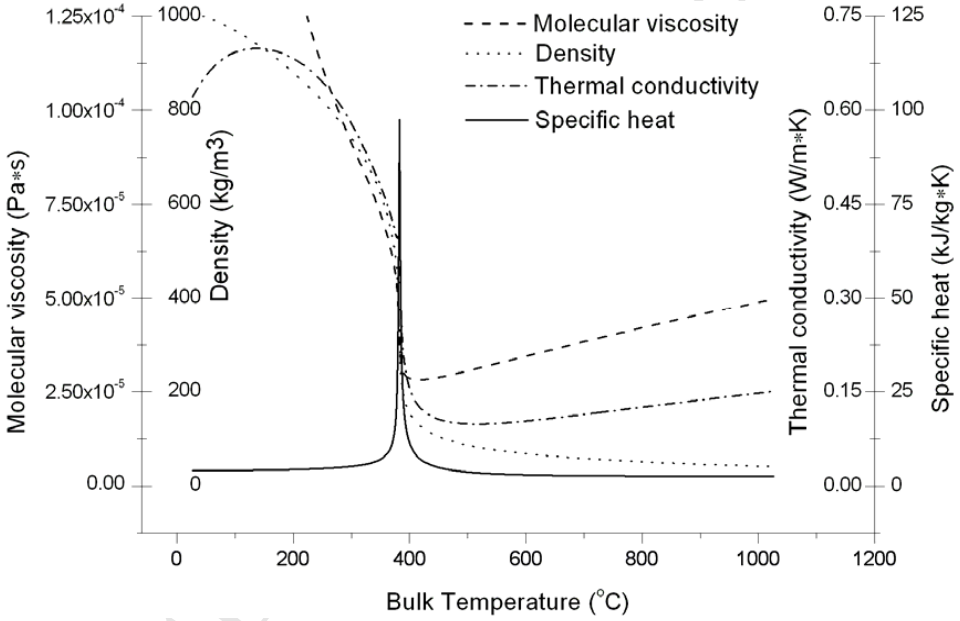

Fig. 1 Variations of thermal-physical properties of SCW at the pressure 24.4MPa

3. Methodology

Because of the special thermal-physical properties of SCW, the flow cannot be treated as a simple incompressible flow with the constant physical properties. Therefore the mass, momentum and energy conservation equations are employed as the following equations.

3.1 Governing equations

$$\frac{\partial \rho}{\partial t}+\frac{\partial \rho u_i}{\partial x_i}=0 \tag{1}$$

$$\frac{\partial \rho u_i}{\partial t}+\frac{\partial \rho u_i u_j}{\partial x_i}=-\frac{\partial p}{\partial x_i}+g_i\left(\rho-\rho_{ref}\right)+\frac{\partial}{\partial x_j}\left[\mu\left(\frac{\partial u_i}{\partial x_j}+\frac{\partial u_j}{\partial x_i}\right)-\frac{2}{3}\mu\frac{\partial u_k}{\partial x_k}\delta_{ij}\right]+s_m \tag{2}$$

$$\frac{\partial \rho h}{\partial t}+\frac{\partial \rho h u_i}{\partial x_i}=\frac{\partial p}{\partial t}+u_i\frac{\partial p}{\partial x_i}+\left[\mu\left(\frac{\partial u_i}{\partial x_j}+\frac{\partial u_j}{\partial x_i}\right)-\frac{2}{3}\mu\frac{\partial u_k}{\partial x_k}\delta_{ij}\right]\frac{\partial u_i}{\partial x_j}+\frac{\partial}{\partial x_i}\left(\alpha\frac{\partial T}{\partial x_i}\right)+s_h \quad (3)$$

where the relationship connected between enthalpy and temperature is given as $h=c_pT-c_{pref}T_{ref}$. For turbulent flow, the corresponding turbulence model is employed to describe the effects of the turbulent fluctuations.

3.2 Turbulence modelling

When the flow is turbulent, the source terms in equation (2) and (3) can be defined as the following formulas modeled as Reynolds stress and turbulent diffusion flux of enthalpy.

$$s_m=-\frac{\partial}{\partial x_j}\left(\overline{\rho u_i' u_j'}\right) \quad (4)$$

$$s_h=-\left(\overline{\rho u_i' u_j'}\right)\frac{\partial u_i}{\partial x_j}-\frac{\partial \overline{\rho u_i' h'}}{\partial x_i} \quad (5)$$

where $\overline{\rho u_i' h'}=-\frac{\mu_t}{\sigma_h}\frac{\partial h}{\partial x_i}$ and the Reynolds stress term, $\overline{\rho u_i' u_j'}$, can be presented by the turbulence models.

The former researches indicated that the choice of the turbulence model is a key issue for SCW simulations. After studying the two dimensional tube flows, in [11] it was found that the turbulence models having the anisotropic characters would give more accurate predictions. The influence of the near wall mesh partitions was also studied in [11]. It concluded that the y^+ value near wall should be less than 1 when RANS (Reynolds Average Navier-Stokes) turbulence models are employed for SCW. In [12] it studied the sub-channels of triangle and square rod bundles and found the non-uniform distribution of the wall temperature along the circumferential perimeter using the SSG (the Reynolds Stress model of Speziale, Sarkar and Gatski) turbulence model that has the anisotropic characters. In [13] it employed different turbulence models to compare the CFD results with experiments and had the conclusion that high Reynolds number k-ε turbulence model with the Hassid and Poreh near-wall treatment would give more accurate simulations than low Reynolds number k-ε turbulence model and k-ω turbulence model.

In [9] it studied the horizontal tubes compared with the experiments in [6] and found the Speziale non-linear high Reynolds k-ε turbulence model with the Hassid and Poreh near-wall treatment under $y^+ < 1.0$ can give good predictions of the heat transfer of SCW using STAR-CD code. In this paper, the mesh partition method (stretched mesh near wall and general structure mesh inside main flow domain), y^+ value and the Speziale non-linear high Reynolds k-ε turbulence model with the Hassid and Poreh near-wall treatment are adopted same as in [9, 14-15].

The Speziale non-linear high Reynolds k-ε turbulence model can be presented by the turbulence kinetic energy and the turbulence dissipation rate in [16] equations as the followings.

$$\frac{\partial \rho k}{\partial t}+\frac{\partial \rho k u_i}{\partial x_i}=\mu_t\left(S_{ij}\frac{\partial u_i}{\partial x_j}-\frac{g_i}{\rho\sigma_h}\frac{\partial \rho}{\partial x_i}\right)-\rho\varepsilon-\frac{2}{3}\left(\mu_t\frac{\partial u_i}{\partial x_i}+\rho k\right)\frac{\partial u_i}{\partial x_i}+\mu_t P_{NL}+\frac{\partial}{\partial x_i}\left[\left(\mu+\frac{\mu_t}{\sigma_k}\right)\frac{\partial k}{\partial x_i}\right] \quad (6)$$

$$\frac{\partial \rho\varepsilon}{\partial t}+\frac{\partial \rho\varepsilon u_i}{\partial x_i}=C_{\varepsilon 1}\frac{\varepsilon}{k}\left[\mu_t S_{ij}\frac{\partial u_i}{\partial x_j}-\frac{2}{3}\left(\mu_t\frac{\partial u_i}{\partial x_i}+\rho k\right)\frac{\partial u_i}{\partial x_i}\right]-C_{\varepsilon 2}\rho\frac{\varepsilon^2}{k}- C_{\varepsilon 3}\mu_t\frac{\varepsilon}{k}\frac{g_i}{\rho\sigma_h}\frac{\partial \rho}{\partial x_i}+C_{\varepsilon 4}\rho\varepsilon\frac{\partial u_i}{\partial x_i}+C_{\varepsilon 1}\mu_t\frac{\varepsilon}{k}P_{NL}+\frac{\partial}{\partial x_i}\left[\left(\mu+\frac{\mu_t}{\sigma_\varepsilon}\right)\frac{\partial \varepsilon}{\partial x_i}\right] \tag{7}$$

where $S_{ij}=\frac{\partial u_i}{\partial x_j}+\frac{\partial u_j}{\partial x_i}$, $P_{NL}=-\frac{\rho}{\mu}\overline{u_i'u_j'}\frac{\partial u_i}{\partial x_j}-\left[S_{ij}\frac{\partial u_i}{\partial x_j}-\frac{2}{3}\left(\frac{\partial u_i}{\partial x_i}+\frac{\rho k}{\mu}\right)\frac{\partial u_i}{\partial x_i}\right]$ and $\mu_t=\frac{C_\mu\rho k^2}{\varepsilon}$. Table 1 gives the corresponding constant coefficients for the Speziale non-linear high Reynolds k-ε turbulence model.

Table 1 Coefficients of the Speziale non-linear high Reynolds k-ε turbulence model

C_μ	σ_k	σ_ε	σ_h	$C_{\varepsilon 1}$	$C_{\varepsilon 2}$	$C_{\varepsilon 3}$	$C_{\varepsilon 4}$
0.09	1.0	1.219	0.9	1.44	1.92	1.44	-0.33

Normally, the high Reynolds k-ε turbulence models employ wall functions to avoid directly describing the fluid flow near wall where $y^+ < 10.0$ in [17]. For dealing with this issue, STAR-CD uses some one-equation turbulence models to perform the simulations for the regions of $y^+ < 10.0$. Through the sensitive studies of the one-equation turbulence models for the heat transfer of SCW, in [9] it indicated that the Hassid and Poreh in [18] model would be the best to describe the flow and heat transfer of SCW within the near wall regions. This one-equation mode calculates the turbulence kinetic energy k from the transport equation like equation (6) and the turbulence dissipation rate ε is gotten from an algebraic function as the following.

$$\varepsilon=\frac{k^{3/2}}{l}\left(0.164 f_\mu+\frac{0.336}{\mathrm{Re}_l}\right) \tag{8}$$

where $f_\mu=1-e^{\left(-\frac{1}{34.48}\mathrm{Re}_l\right)}$, $\mathrm{Re}_l=\frac{\sqrt{k}l}{\nu}$ and $l=0.419y$, where y is the normal distance from the wall.

3.3 Numerical method

Through the tests, it is found that the steady and unsteady simulations for the horizontal tubes can reach the same results finally. However the unsteady calculation will spend longer time than the steady computation. Therefore, in this paper, all the simulations are based on the steady calculation. It means all the temporal terms in the equations (1, 2, 3, 6 and 7) can be treated as 0, i.e., $\partial\phi/\partial t=0$.

The finite volume scheme is employed to do the spatial discretization. Generally, the differential manner of the convective and diffusive fluxes will affect the numerical accuracy and stability. As usual CFD applications, the central differential scheme for the diffusive fluxes is employed. It is difficult for the convective fluxes to keep a high differencing accuracy meanwhile preserving the numerical stability especially for the sharp changes of the physical properties like SCW around the pseudo-critical temperature in Fig. 1. The following convective differencing schemes, shown in Table 2, will be tested in this paper. In Table 2, CD means the central differencing, LUD means linear upwind differencing and MARS is abbreviatory for Monotone Advection and Reconstruction Scheme. QUICK is of the quadratic upstream interpolation of convective kinematics.

Table 2 Convective differencing discretization schemes

Cases	Discretization scheme	Accuracy of differencing scheme
1	CD	second order
2	LUD	second order
3	MARS	second order
4	QUICK	third order

In the practical numerical application, QUICK scheme uses two points upstream and one point downstream to get the interpolated value. If the grid is skewed, it has the potential risk to have the numerical dispersion in [17]. The other three schemes have the same accurate order. LUD is derived from a scheme originally proposed for structure meshes. Same as QUICK scheme it can produce solutions that are outside the physical bounds on ϕ in [17]. CD simply interpolates linearly on the nearest neighbor grids without considering the flow direction. This scheme produces less numerical diffusion, but can be dispersive potentially in [17]. MARS does not rely on any problem dependent parameters to work properly and it can automatically deal with all flow problems. Of all schemes available in STAR-CD, MARS possesses the least sensitivity of solution accuracy to the mesh structure and skewness in [17].

After deciding the differencing scheme, the last issue for the numerical method is the solution algorithm. Here SIMPLE algorithm in [19] is chosen for the steady flow situation and PISO algorithm in [20] is used for the transient (unsteady) flow regime. During the simulation, the default settings in the code are adopted. The CG (conjugate gradient) method in [21] is used to solve the final linear algebraic equations.

4. Physical problem and computational conditions

Fig. 2 shows the schematic geometry. The computational test parameters are used same as the experiments in [6].

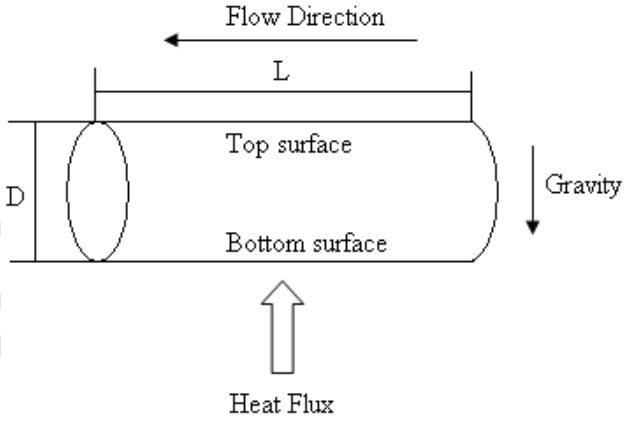

Fig. 2 Schematic geometry of flow system

In the geometry sketch, L is the tube length and D is the tube diameter. The supercritical water with the system pressure 24.4MPa enters into the tube from the right-hand-side, flows out from the left-hand-side and is heated by the tube wall same as the experiment. The flow direction is normal to the gravity.

In the former studies, in [9] it used different meshes to test the horizontal tube and found the suitable mesh partitions. In this paper, mesh partitions near wall are same as in [9] keeping $y^+ < 1.0$. In the practice, the specific mesh partitions are found by the mesh sensitive studies for every individual diameter.

The boundary conditions for the round tube are straightforward. The inlet keeps the uniform mass flux and the wall boundary with a uniform heat flux. The default outlet settings of STAR-CD code are adopted at the outlet.

5. Discretization scheme tests

The mass flux of 340kg/m^{2}s and the wall heat flux of 300kW/m^2 are used as the flow parameters for the discretization scheme influence studies. They are same as the experiment in [6]. In the experiment, the round tube is L=3m long with the inner diameter D=6.3mm. Fig. 3 shows the numerical results of the 4 cases in Table 2 compared with the experiment data.

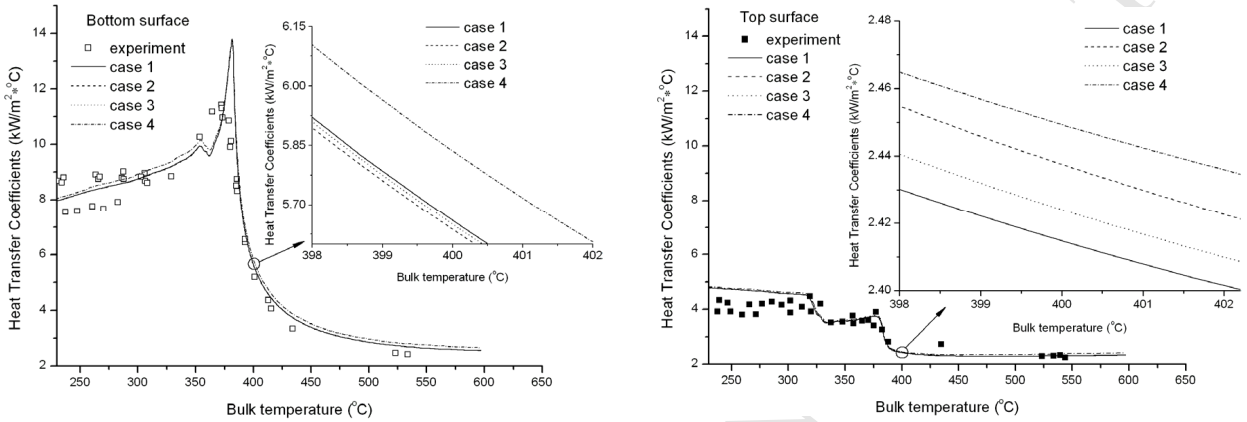

(a) At bottom surface (b) At top surface

Fig. 3 Comparisons of discretization scheme influence on heat transfer coefficients

From Fig. 3, it can be seen that QUICK scheme (case 4) departures from experiments more than the others especially when the bulk temperature, which is the average fluid temperature at the corresponding cross section vertical to the tube axes, is greater than 400^{o}C at the bottom surface. At the top surface, all of the schemes get the similar accurate results. The errors of CD and LUD schemes are within ±1% using MARS scheme as the reference. However, QUICK scheme has the maximum error exceeds 5%. It can be seen that differencing discretization schemes are not sensitive to the numerical simulations for the flow and heat transfer of SCW, just among CD, LUD and MARS schemes. The MARS scheme will be employed in this paper for the late case studies.

6. Results and Discussions

After the discretization scheme tests, the formal studies of the diameter effects on the heat transfer are carried out. Table 3 shows the corresponding cases. The mesh sensitivity studies are carried out for all the cases to get the mesh independent results as in [9, 14-15].

Table 3 Flow conditions of simulation cases

Cases	System pressure	Mass flux	Heat flux	Diameters
5 – 10	24.4 MPa	340 kg/m^{2}s	300 kW/m^2	5 – 10 mm
11 –16	24.4 MPa	964 kg/m^{2}s	307 kW/m^2	5 – 10 mm

6.1 Low mass flux regime

The low mass flux regime (340 kg/m^{2}s) of case 5-10 in Table 3 is firstly studied. Fig. 4 shows the variations of the wall temperature against the bulk enthalpy at different diameters from 5mm to 10mm. All the curves of the wall temperature at the bottom surface almost collapse together in Fig. 4(a). They have the same shapes and tendencies. When the bulk enthalpy is less than 1750kJ/kg (365.42^{o}C), the wall temperature ascends

pseudo-linearly following the enthalpy increase. The wall temperature curves become flat between 1750kJ/kg (365.42°C) and 2250kJ/kg (383.95°C) because this enthalpy gap just covers over the pseudo-critical point (2143.59kJ/kg, 382.7°C), in Fig. 1. The big specific heat capacity (c_p) will allow SCW to absorb lots of heat without the evident temperature increase. This phenomenon is quite like the boiling heat transfer that the heat is absorbed by the liquid to generate the vapor rather than to increase the temperature in [22]. Therefore the tube wall temperature does not increase evidently. When the bulk enthalpy greater than 2250kJ/kg, the specific heat (c_p) of SCW falls down. The fluid losses the capacity absorbing heat. It cannot cool down the tube wall enough. Hence the wall temperature increases again. However, in Fig. 4(b) the situation of the top surface is totally different from the bottom surface. When the diameter is greater than 8mm, the wall temperature has an abrupt local peak. It can be seen that the local peak locates around the pseudo-critical point. This abrupt peak is caused by the heat transfer deterioration, shown in Fig. 5.

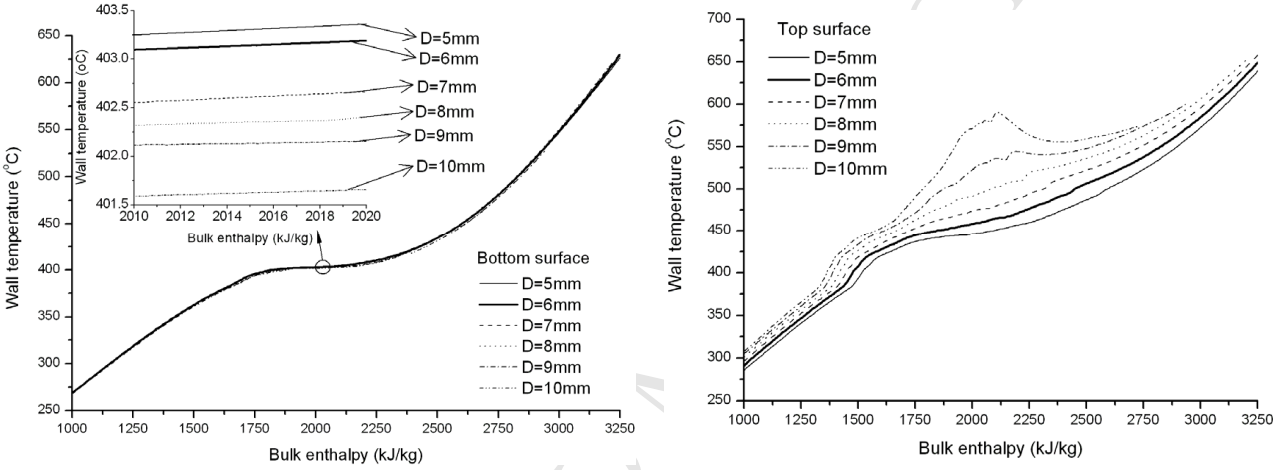

(a) At bottom surface (b) At top surface

Fig. 4 Comparisons of different diameter influence on wall temperature

Fig. 5 shows the variations of the heat transfer coefficients. From Fig. 5, it can be seen that the heat transfer coefficients decrease following the diameter increase. The values of heat transfer coefficients around the pseudo-critical temperature not only reduce the amplitude but also turn down to the valley following the increase of the diameter. This phenomenon is called as the heat transfer deterioration.

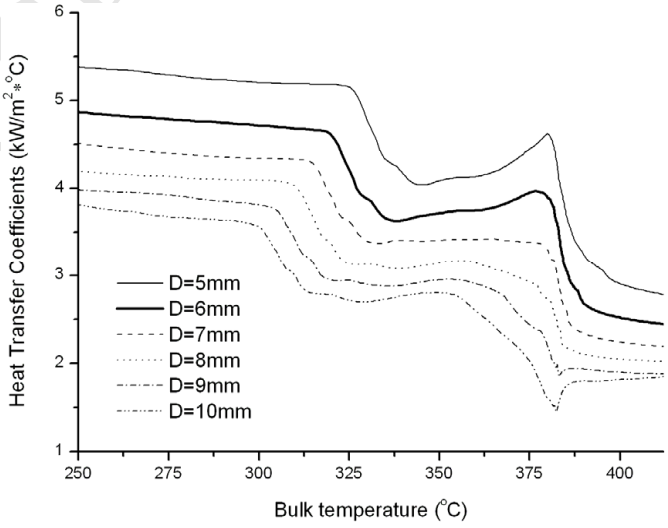

Fig. 5 Heat transfer coefficients at top surface

Due to the buoyancy, the fluid near the tube wall is driven by the buoyancy to flow up. However, at the same time the gravity tries to drive the fluid to flow downward from the top to the bottom. Ultimately the fluid flows to where will be up to the stronger one. Due to the stronger buoyancy in large diameter tube, seen in Fig. 6, when the fluid reaches the upper domain the gravity, comparing with buoyancy, is not strong enough to drive the fluid down. However, because of the blockage of the top wall, the fluid cannot be driven flowing up anymore. Finally the fluid is stopped at the upper domain of the tube to generate a stagnant flow. The stagnation flow cannot provide the convection heat transfer to take away the accumulated heat. Therefore it will lead the temperature ascending. For an extreme, it can make the wall temperature to increase abruptly, shown in Fig. 4(b).

Usually the Gr/Re^2 ratio is employed to quantify the buoyancy effect in [6]. Once it has the order of unity or higher, the buoyancy effect cannot be neglected. In physics, the ratio represents the competition between the buoyancy and inertia forces. The greater the ratio value the stronger the buoyancy effect. The definition of the Gr number uses the following formula that considers the temperature gradient variations inside the flow field.

$$Gr = \frac{g\beta_b D^4}{\nu_b^2}|\nabla T| \tag{9}$$

where β is the bulk thermal expansion and ν is the kinematic viscosity of SCW. Subscript b delegates bulk temperature. The Re number is defined as the usual formula as $\mathrm{Re}_b = \rho_b VD/\mu_b$.

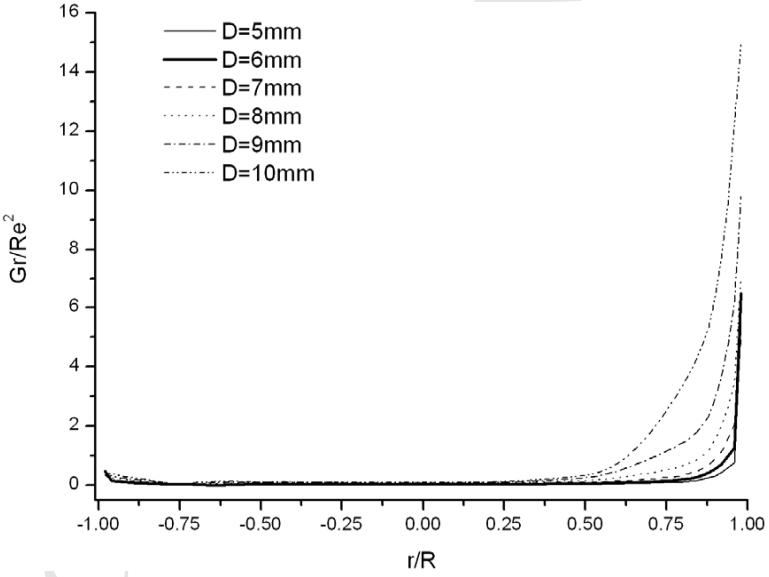

Fig. 6 Gr/Re^2 ratio comparisons at low mass flux

Fig. 6 shows the Gr/Re^2 ratio comparisons curves of different tubes at the cross section with the bulk enthalpy of 2111.74kJ/kg (382.4^{o}C). From Fig. 6, it can be seen that near the bottom surface (r/R = -1) all the Gr/Re^2 ratios of the tubes are less than 1. It means the buoyancy effect on the heat transfer can be ignored. However, near the top surface (r/R = 1), the Gr/Re^2 ratios are larger than 1. It means there are strong buoyancy effects around the top surface.

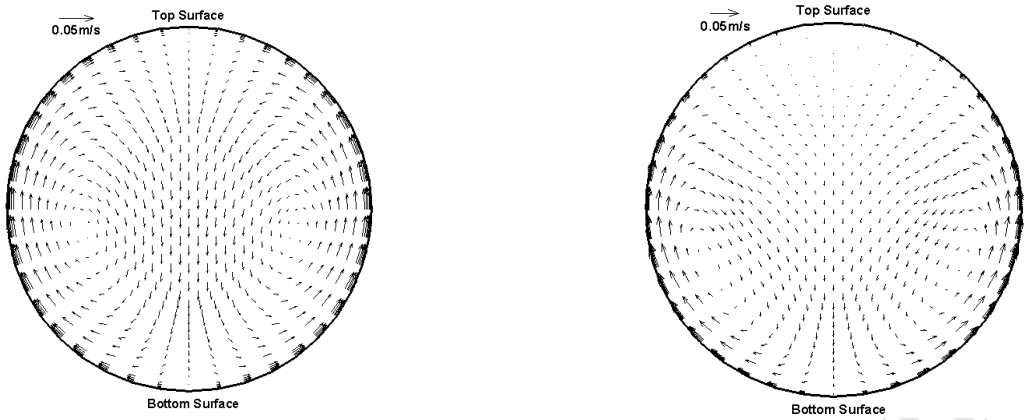

(a) D=5mm (b) D=10mm

Fig. 7 Convective flow at the cross section of the pseudo-critical temperature

The buoyancy not only affects the heat transfer but also affects the secondary flow patterns as well. Fig. 7 shows the velocity vectors of the secondary convective flow of the cross section at the pseudo-critical temperature where the bulk temperature equals to the pseudo-critical temperature (382.7^{o}C). These two velocity vectors are different. From Fig. 7, it can be seen that at large diameter (D=10mm) the circumfluence locates at the lower part of the tube and the centers of the circumfluence are near the wall. A wide stagnation domain can be observed for the large diameter of D=10mm near the top region.

Fig. 8 shows the comparisons between the CFD results and the classical theoretical predictions. Here the Dittus-Boelter formula for single phase fluids shown in equation (10) is chosen as the theoretical prediction formula in [23].

$$Nu = 0.023\,\mathrm{Re}_b^{0.8}\,\mathrm{Pr}_b^{0.4} \tag{10}$$

where Nu is Nusselt number and Pr_b is Prandtl number of the fluid at the bulk temperature.

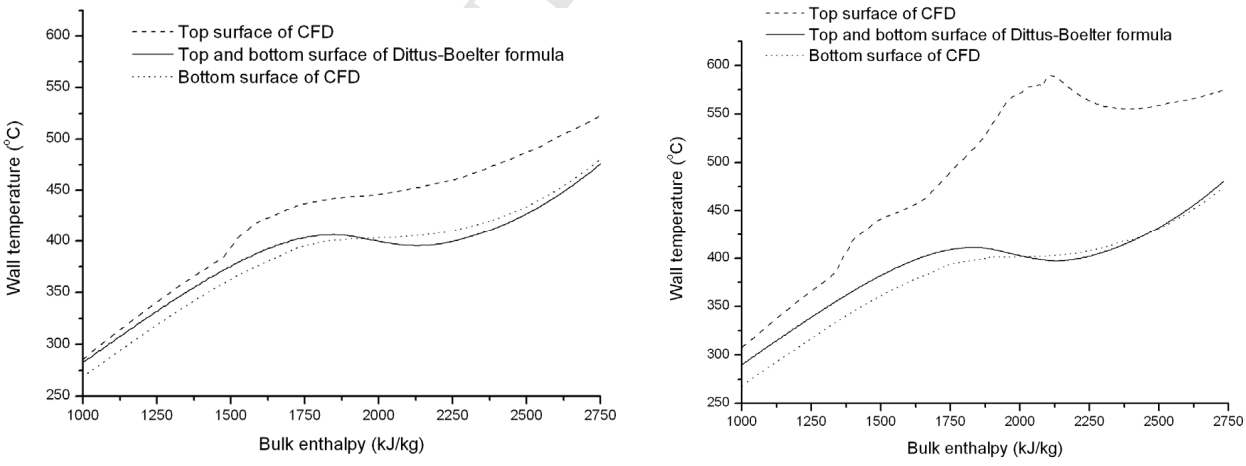

(a) D=5mm (b) D=10mm

Fig. 8 Comparisons between CFD and classical theoretical prediction

From Fig. 8, it can be seen, the differences between Dittus-Boelter formula and CFD are smaller at the bottom surface. However, at the top surface, the predictions of Dittus-Boelter formula are quite different from CFD results. The reason is because Dittus-Boelter formula does not consider the buoyancy effects.

6.2 High mass flux regime

As the former studies for the horizontal tubes, the high mass flux situation is also studied in this paper using cases 11-16 in Table 3. In [6] it declared that at the conditions of mass flux of 964kg/m^{2}s and heat flux of 307kW/m^2 the buoyancy effect can be negligible. In [9] it studied this flow condition at different system pressures and also found the heat transfer characters of the high mass flux were different from the low mass flux. Therefore it is necessary to do the studies of the diameter effects for the horizontal tubes of SCW at high mass flux. Here the conditions of mass flux of 964kg/m^{2}s and heat flux of 307kW/m^2 are kept same as the high mass flux regime in [6, 9].

Fig. 9 shows the variations of the heat transfer coefficients at different diameters. From the comparisons, it can be seen that the top surface and the bottom surface have the similar variations of the heat transfer coefficients. It is only the heat transfer coefficients at the bottom surface are more concentrated than the top surface especially when the bulk temperature is less then the pseudo-critical temperature. The small diameter has the higher heat transfer coefficients.

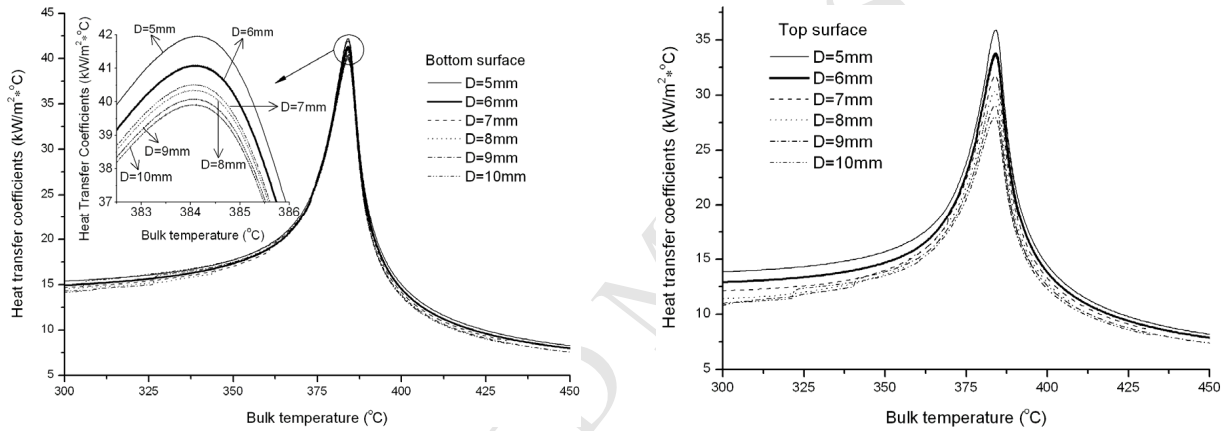

(a) At bottom surface (b) At top surface

Fig. 9 Comparisons of different diameter influence on heat transfer coefficients

Fig. 10 shows comparisons between the CFD simulation results and Dittus-Boelter predictions. From the comparisons, it can be seen that the CFD results are coincident very well to the theoretical predictions of Dittus-Boelter formula at both of the surfaces. This improves buoyancy is unable to affect the high mass flux on the heat transfer.

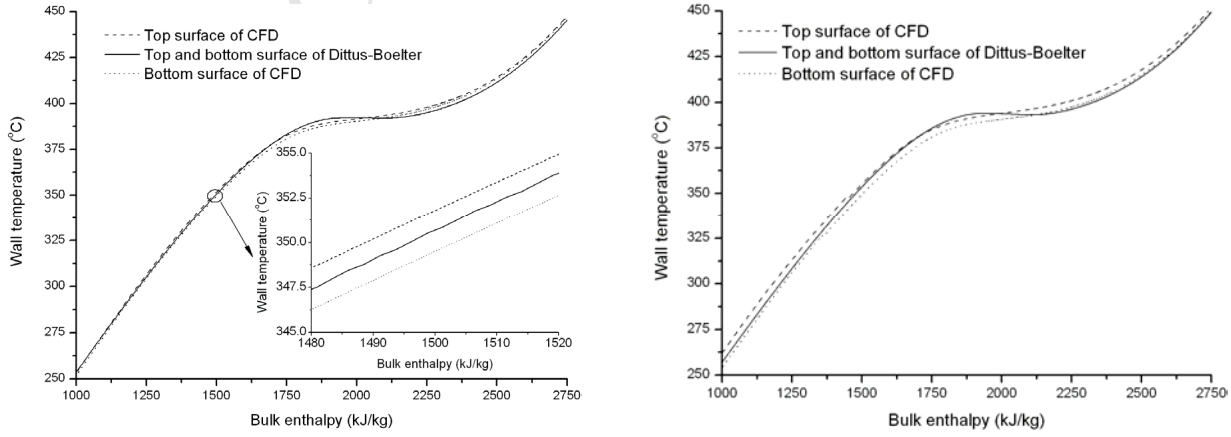

(a) D=5mm (b) D=10mm

Fig. 10 Comparisons between CFD and Dittus-Boelter formula

In [6, 9] it found the high mass flux would induce weak buoyancy effects. Here the quantificational analysis of the Gr/Re^2 ratio shown in Fig. 11 will help to understand the weak buoyancy effect of the high mass flux. Fig. 11 shows the Gr/Re^2 ratio comparisons for different tubes at the bulk enthalpy of 2143.59kJ/kg (382.7^{o}C). It can be seen that all the Gr/Re^2 ratios are much less than 1. This means the high mass flux can eliminate the buoyancy effects.

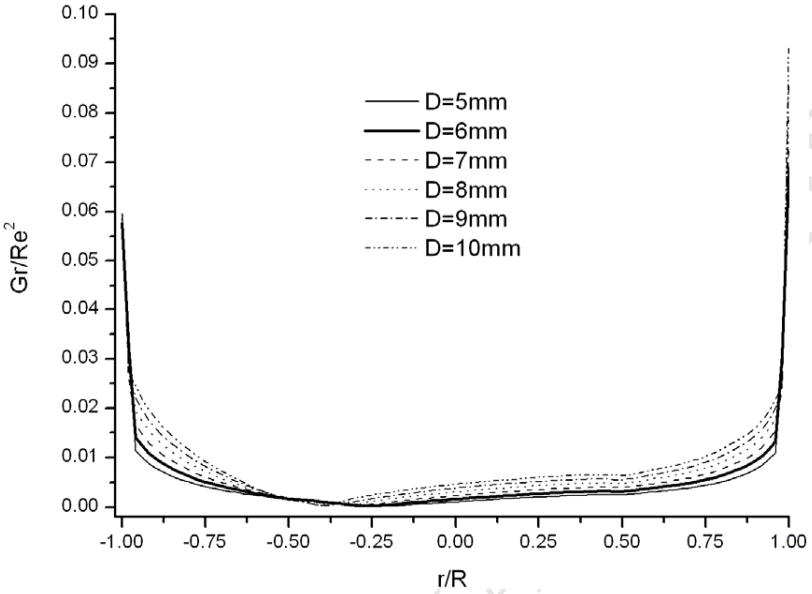

Fig. 11 Gr/Re^2 ratio comparisons at high mass flux

6.3 Circumference distributions of wall temperature

According to the practical engineering design, the tube wall temperature distribution is one of the critical criteria for the safe operations in [6, 9, 12-13]. Therefore it is necessary to know the wall temperature distributions along the circumference. Fig. 12 shows wall temperature distributions along the circumference for different diameters at both regimes of low and high mass flux. The cross sections are at the bulk enthalpy of 2111.74kJ/kg (382.4^{o}C) for the low mass flux regime and the pseudo-critical bulk enthalpy of 2143.59kJ/kg (382.7^{o}C) for the high mass flux regime. The θ direction starts from the bottom surface, turns to the top surface following counter-clockwise from 0^o to 360^o.

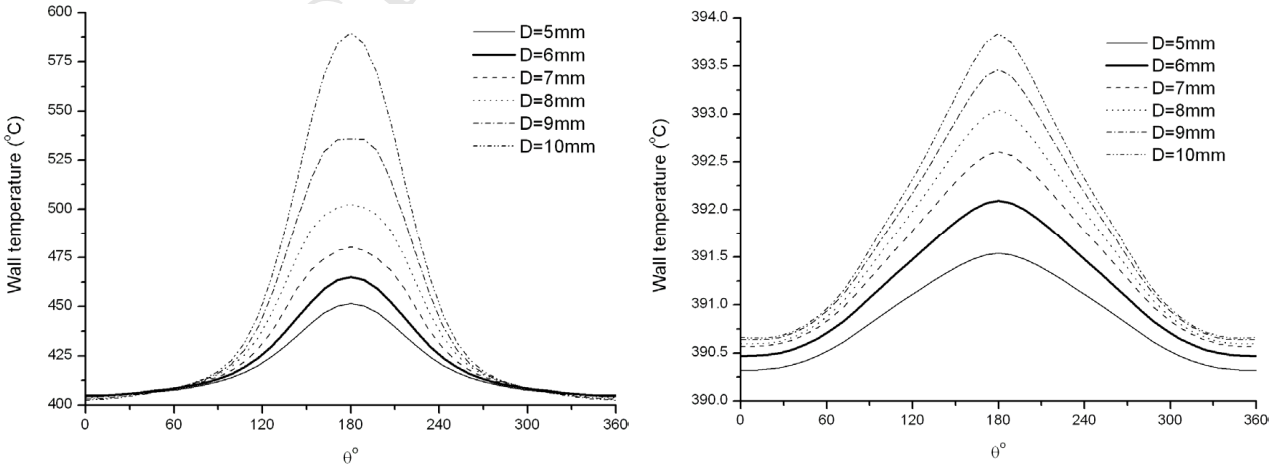

(a) Low mass flux (b) High mass flux

Fig. 12 Wall temperature distributions along circumference

It can be seen in Fig. 12(a), the strong buoyancy effect at the low mass flux can introduce the wall temperature difference between the top surface and the bottom surface to 180^{o}C high at D=10mm. Such high wall temperature difference comparing with the difference only 3^{o}C at the high mass flux regime in Fig. 12(b) should be a potential crisis to the safe operations of the facilities especially nuclear reactors. However, if the strong buoyancy effects were employed to drive the fluid flows for instance the passive natural circulation, the consequence would be considerably tremendous.

7. Conclusions

The heat transfer characteristics of SCW can be affected by many influence factors, such as geometry sizes, flow conditions and driven forces. A good understanding to these influences is very important for the facilities (e.g. SCWR) which use SCW as the refrigerant. Following the previous works in [6, 9], this paper extends the research focus on the diameter effect on the heat transfer. Through the studies, it is found when the mass flux is low the diameter will strongly affect the heat transfer and wall temperature for the horizontal tubes due to the buoyancy effects. Except this, the following observations can be made:

(1) Through the tests, the convective differencing discretization schemes are not sensitive for the flow and heat transfer of SCW among CD, LUD and MARS. In practice, MARS scheme in STAR-CD is recommended.

(2) The diameter has the great influences on the heat transfer for the low mass flux regime. The small diameter is helpful to reduce the buoyancy effect and to enhance the heat transfer. The wall temperature difference increase following the increase of the tube diameter. The strong buoyancy can generate a large wall temperature difference.

(3) The low mass flux has the risk to introduce the heat transfer deteriorations which hinder the heat transfer for the horizontal tubes. The effects are becoming stronger following the diameter increase. The heat transfer deteriorations not only affect the wall temperature, but also produce different secondary flow patterns at the cross sections for different diameters.

(4) The high mass flux can eliminate the heat transfer deteriorations caused by the buoyancy. At high mass flux regime, the Gr/Re^2 ratios are much less than 1 for all the diameters. Even the heat transfer coefficients can be predicted by the classical theoretical Dittus-Boelter formula.

Acknowledgements

The first author wishes to acknowledge the CD-adapco London Company for providing the software and the technique supports.

References

[1] Y. Matsumura, T. Minowa, B. Potic, et al., Biomass gasification in near- and super-critical water: Status and prospects, Biomass and Bioenergy 29 (2005) 269-292.

[2] Z.R. Zhang, H. Yamaguchi, K. Fujima, et al., Theoretical analysis of a thermodynamic cycle for power and heat production using supercritical carbon dioxide, Energy 32 (2007) 591-599.

[3] D.F. Torgerson, B.A. Shalaby, S. Pang, CANDU technology for generation III+ and IV reactor, Nucl. Eng. Des. 236 (2006) 1565-1572.

[4] M. Mori, W. Maschek, A. Rineiski, Heterogeneous cores for improved safety performance a case study: the supercritical water fast reactor, Nucl. Eng. Des. 236 (2006) 1573-1579.

[5] L.Z. Cao, Y. Oka, Y. Ishiwatari, Z. Shang, Fuel, Core Design and Subchannel Analysis of a Superfast Reactor, Journal of Nuclear Science and Technology 45 (2008) 138-148.

[6] M. Bazargan, D. Fraser, V. Chatoorgan, Effect of buoyancy on heat transfer in supercritical water flow in a horizontal round tube, Journal of Heat Transfer 127 (2005) 897~902.

[7] I.L. Pioro, H.F. Khartabil, R.B. Duffey, Heat transfer to supercritical fluids flowing in channels – empirical correlations (survey), Nucl. Eng. Des. 230 (2004) 69-91.

[8] I.L. Pioro, R.B. Duffey, Experimental heat transfer in supercritical water flowing inside channels (survey), Nucl. Eng. Des. 235 (2005) 2407-2430.

[9] Z. Shang, Y.F. Yao, S. Chen, Numerical investigation of system pressure effect on heat transfer of supercritical water flows in a horizontal round tube, Chemical Engineering Science 63 (2008) 4150-4158.

[10] B. Zhang, J.Q. Shan, J. Jiang, Numerical analysis of supercritical water heat transfer in horizontal circular tube. Progress in Nuclear Energy 52 (2010) 678-684.

[11] F. Roelofs, CFD analyses of heat transfer to supercritical water flowing vertically upward in a tube, 1 December, 2004, NRG rapport 21353/04.60811/P.

[12] X. Cheng, B. Kuang, Y.H. Yang, Numerical analysis of heat transfer in supercritical water cooled flow channels. Nucl. Eng. Des. 237 (2007) 240-252.

[13] J. Yang, Y. Oka, Y. Ishiwatari, J. Liu, J. Yoo, Numerical investigation of heat transfer in upward flows of supercritical water in circular tubes and tight fuel rod bundles, Nucl. Eng. Des. 237 (2007) 420~430.

[14] Z. Shang, CFD investigation of vertical rod bundles of supercritical water-cooled nuclear reactor, Nucl. Eng. Des. 239 (2009) 2562~2572.

[15] Z. Shang, S. Lo, Numerical investigation of supercritical water-cooled nuclear reactor in horizontal rod bundles, Nucl. Eng. Des. 240 (2010) 776~782.

[16] C.G. Speziale, On nonlinear k-l and k-ε models of turbulence, J. Fluid Mech. 178 (1987) 459~475.

[17] CD-adapco, STAR-CD Methodology, STAR-CD Version 4.02, 2006, pp. 2-1~2-31, pp. 4-1~4-8 and pp. 7-1~7-9.

[18] S. Hassid, M. Poreh, A turbulent energy dissipation model foe flows with drag reduction, J. Fluids Eng. 100 (1978) 107~112.

[19] S.V. Patankar, D.B. Spalding, A calculation procedure for heat, mass and momentum transfer in three-dimensional parabolic flows, Int. J. Heat Mass Transfer 15 (1972) 1787~1806.

[20] R.I. Issa, Solution of the implicitly discretised fluid flow equatins by operator-splitting, J. Comp. Phys. 62 (1986) 40~65.

[21] H.P. William, A.T. Saul, T.V. William, P.F. Brian, Fundamentals of aerodynamics, 3rd edition Cambridge University Press, Cambridge, 2007, pp. 515~520.

[22] D.L. Bennett, J.C. Chen, Forced convective boiling in vertical tubes for saturated pure components and binary mixtures, AIChE J. 26 (1980) 454~461.

[23] F.W. Dittus, L.M.K. Boelter, Heat transfer in automobile radiators of the tubular type, University Publications in English, Berkeley, 2 (1930) 443~461.

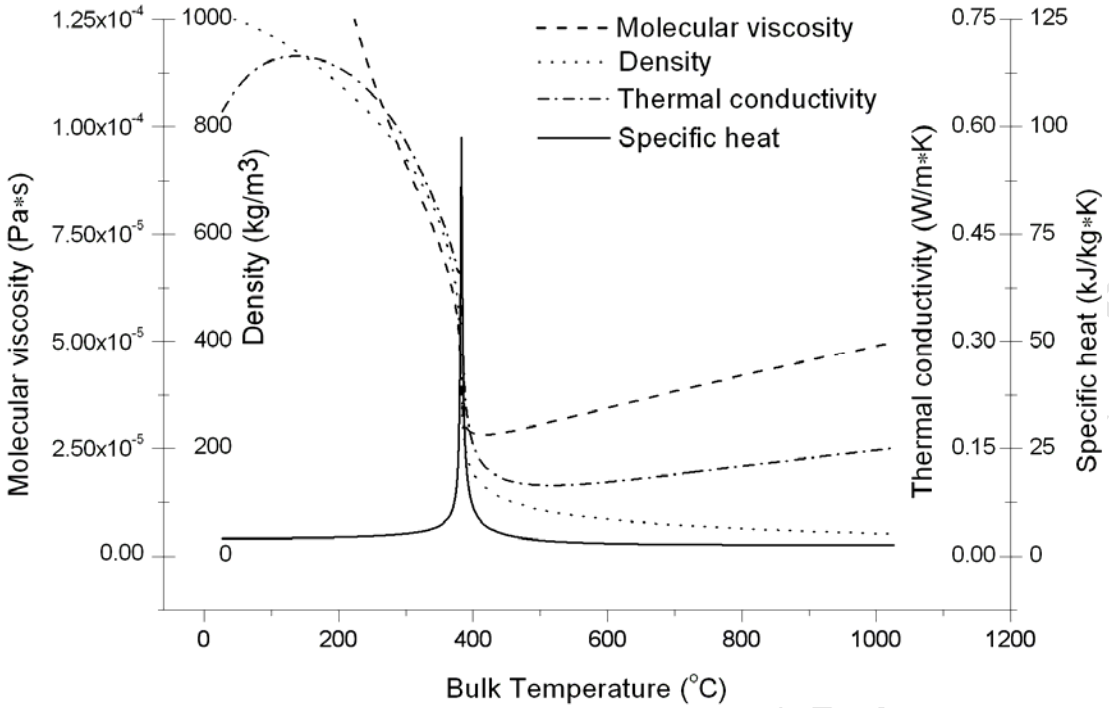

Fig. 1 Variations of thermal-physical properties of SCW at the pressure 24.4MPa

Title of paper: Numerical Investigation of Diameter Effect on Heat Transfer of Supercritical Water Flows in Horizontal Round Tubes

First author: Zhi Shang

The number of figures: 1

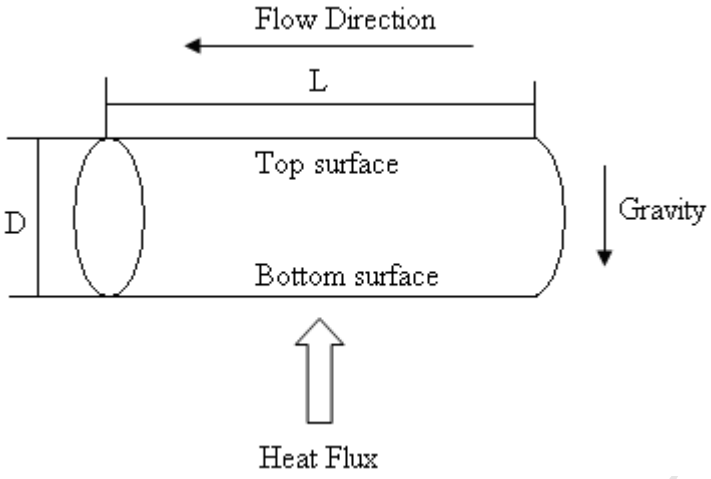

Fig. 2 Schematic geometry of flow systems

Title of paper: Numerical Investigation of Diameter Effect on Heat Transfer of Supercritical Water Flows in Horizontal Round Tubes

First author: Zhi Shang

The number of figures: 2

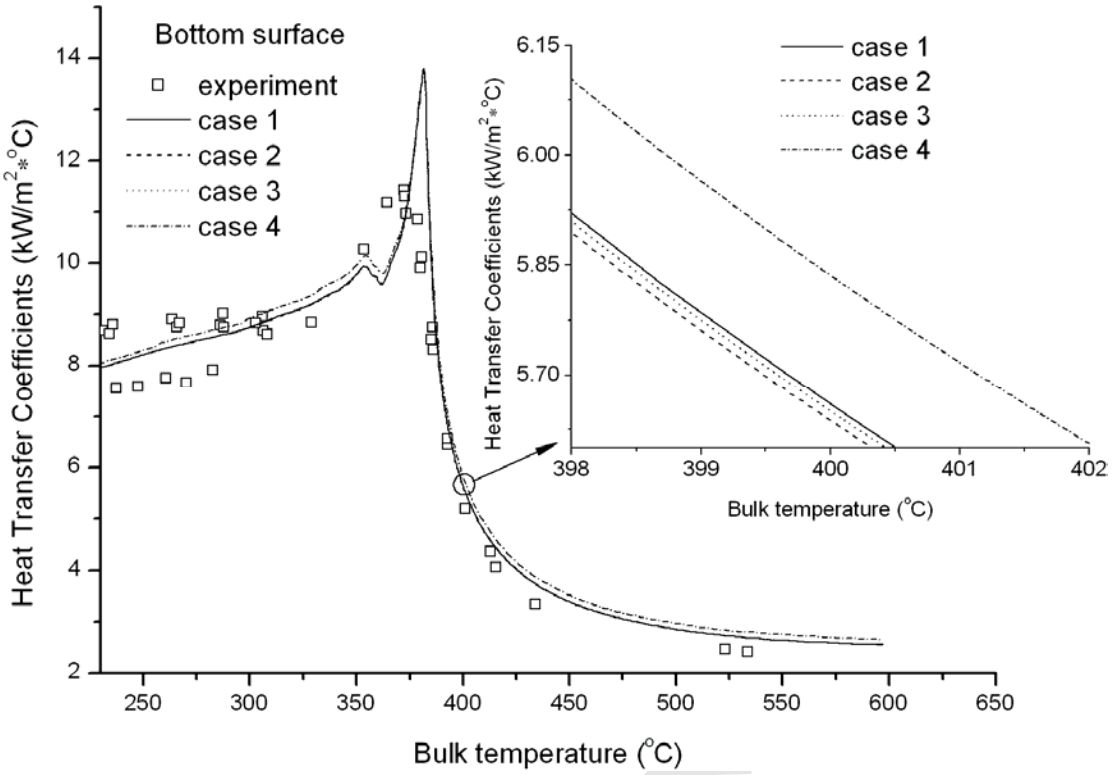

(a) At bottom surface

Fig. 3 Comparisons of discretization scheme influence on heat transfer coefficients

Title of paper: Numerical Investigation of Diameter Effect on Heat Transfer of Supercritical Water Flows in Horizontal Round Tubes

First author: Zhi Shang

The number of figures: 3

The number of sub figures: (a)

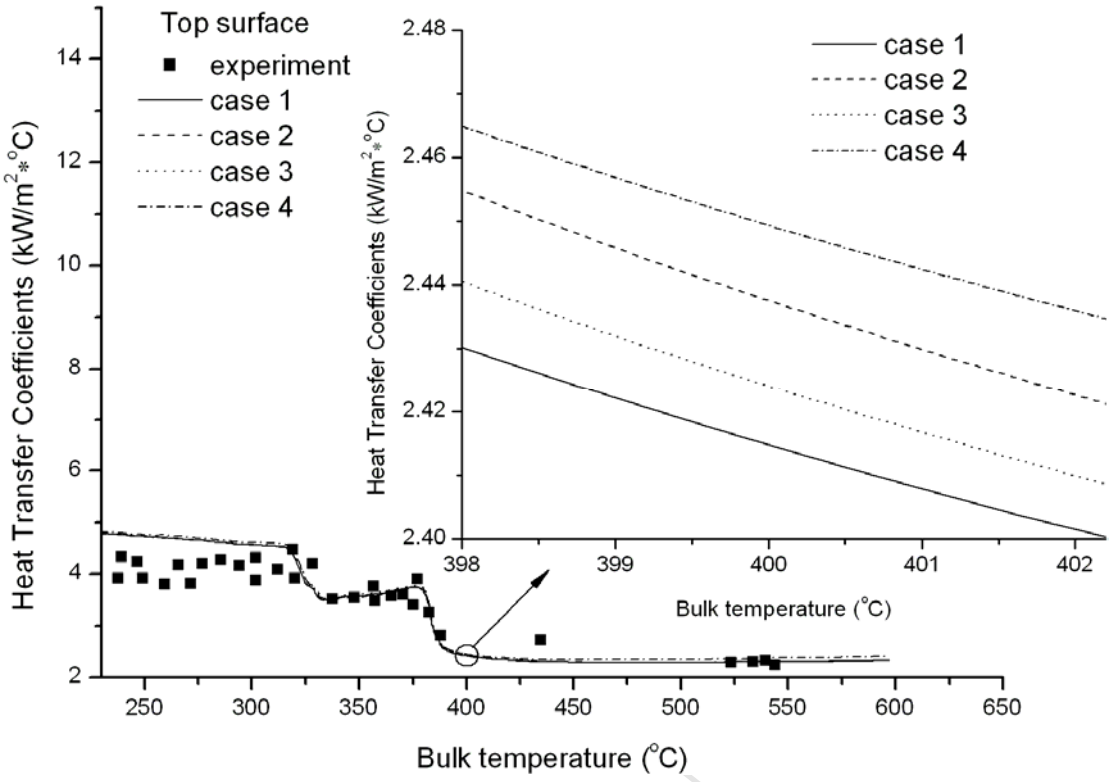

(b) At top surface

Fig. 3 Comparison of discretization scheme influence on heat transfer coefficients

Title of paper: Numerical Investigation of Diameter Effect on Heat Transfer of Supercritical Water Flows in Horizontal Round Tubes

First author: Zhi Shang

The number of figures: 3

The number of sub figures: (b)

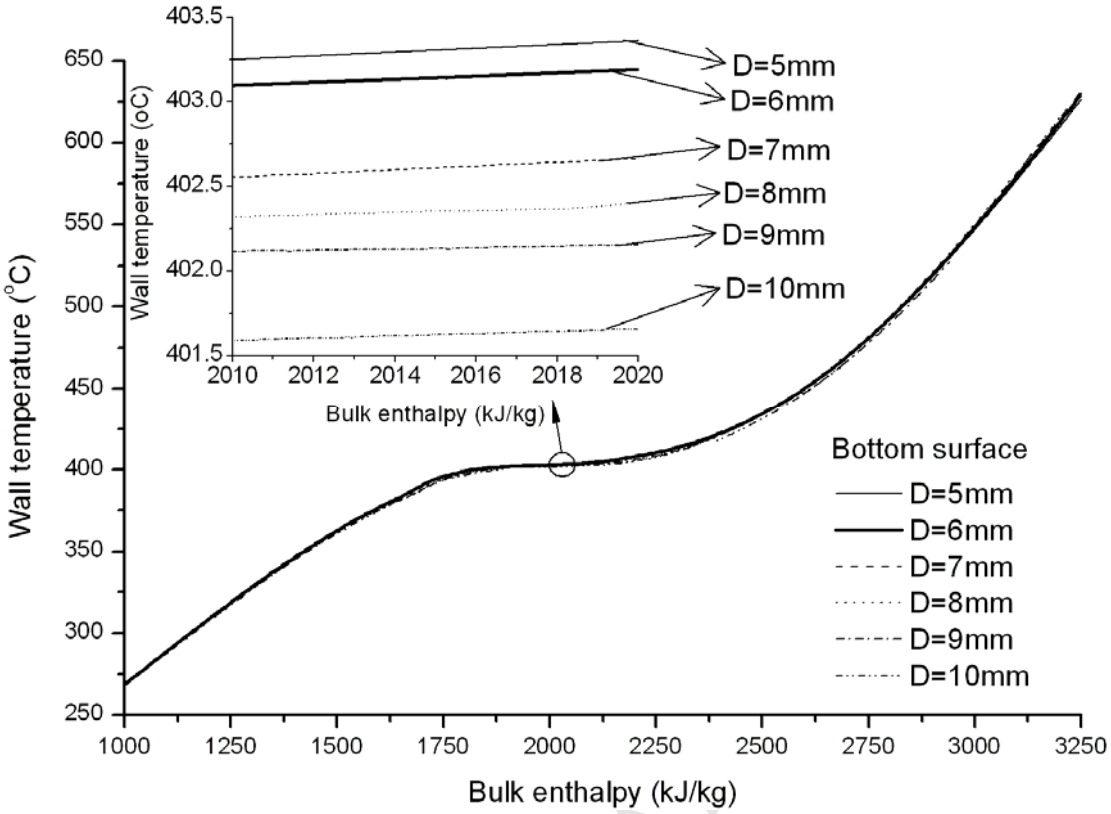

(a) At bottom surface

Fig. 4 Comparison of different diameter influence on wall temperature

Title of paper: Numerical Investigation of Diameter Effect on Heat Transfer of Supercritical Water Flows in Horizontal Round Tubes

First author: Zhi Shang

The number of figures: 4

The number of sub figures: (a)

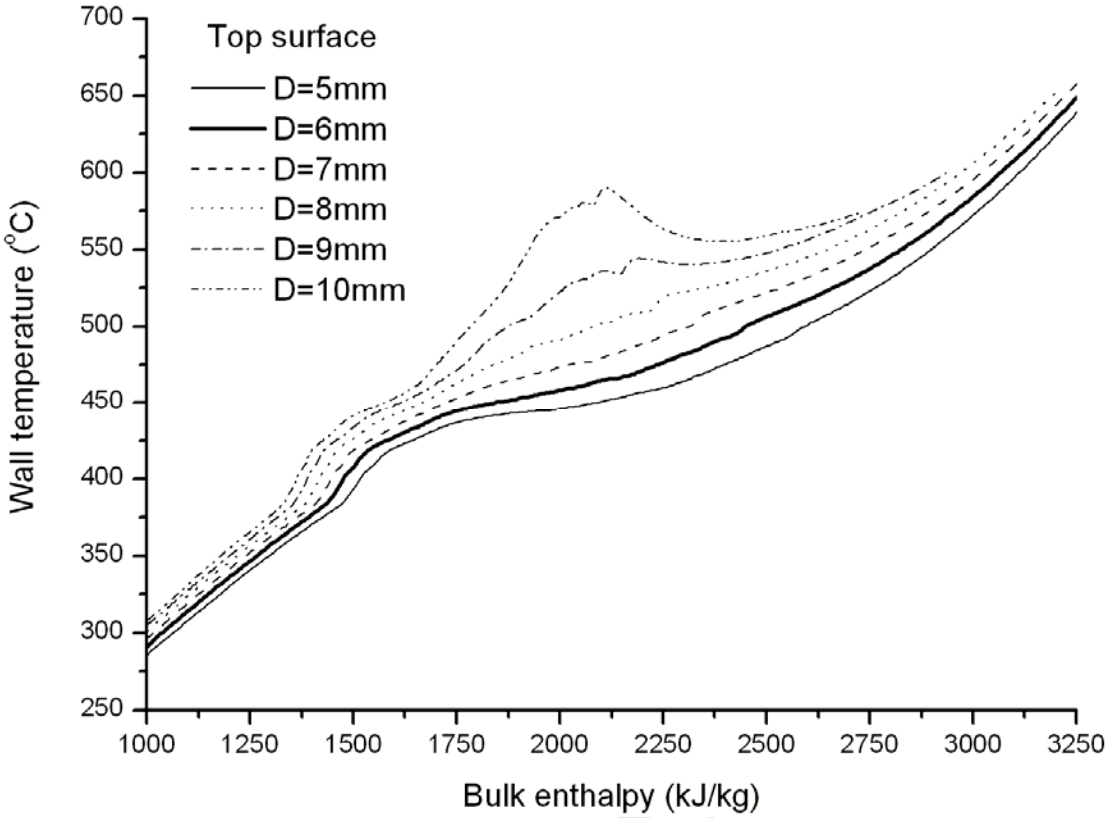

(b) At top surface

Fig. 4 Comparison of different diameter influence on wall temperature

Title of paper: Numerical Investigation of Diameter Effect on Heat Transfer of Supercritical Water Flows in Horizontal Round Tubes

First author: Zhi Shang

The number of figures: 4

The number of sub figures: (b)

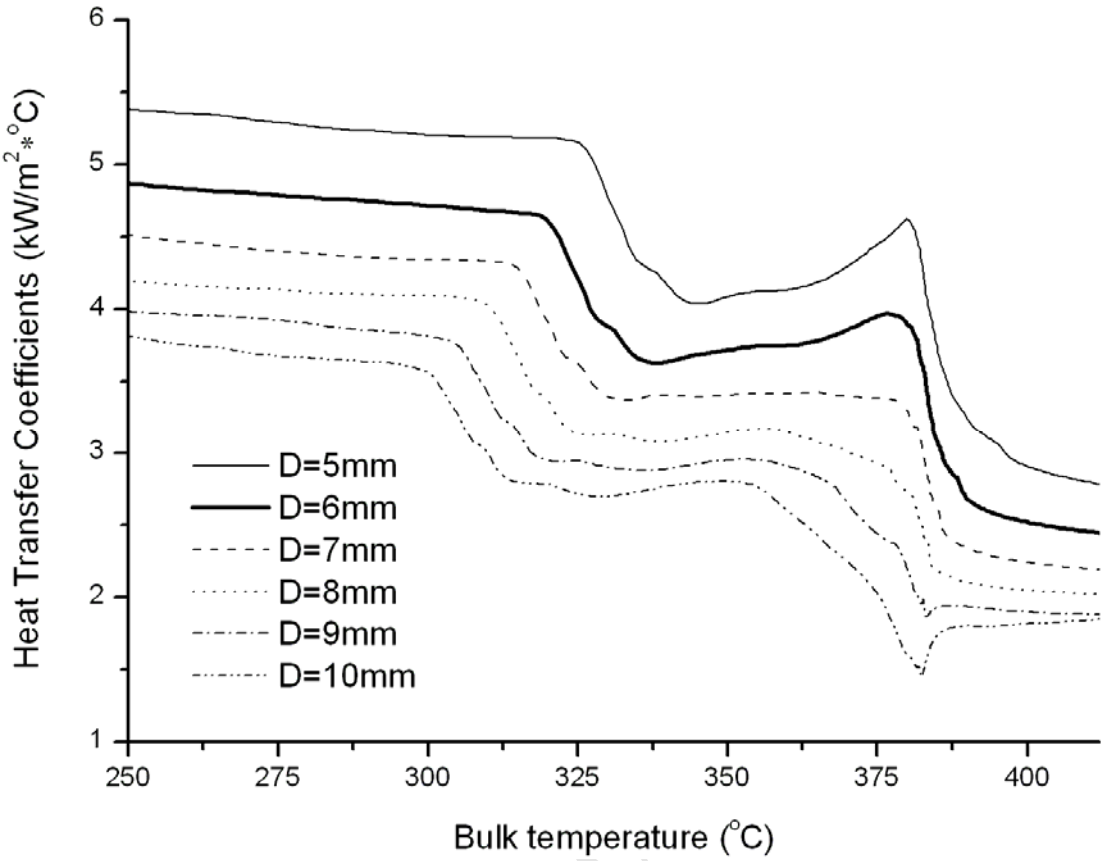

Fig. 5 Heat transfer coefficients at top surface

Title of paper: Numerical Investigation of Diameter Effect on Heat Transfer of Supercritical Water Flows in Horizontal Round Tubes

First author: Zhi Shang

The number of figures: 5

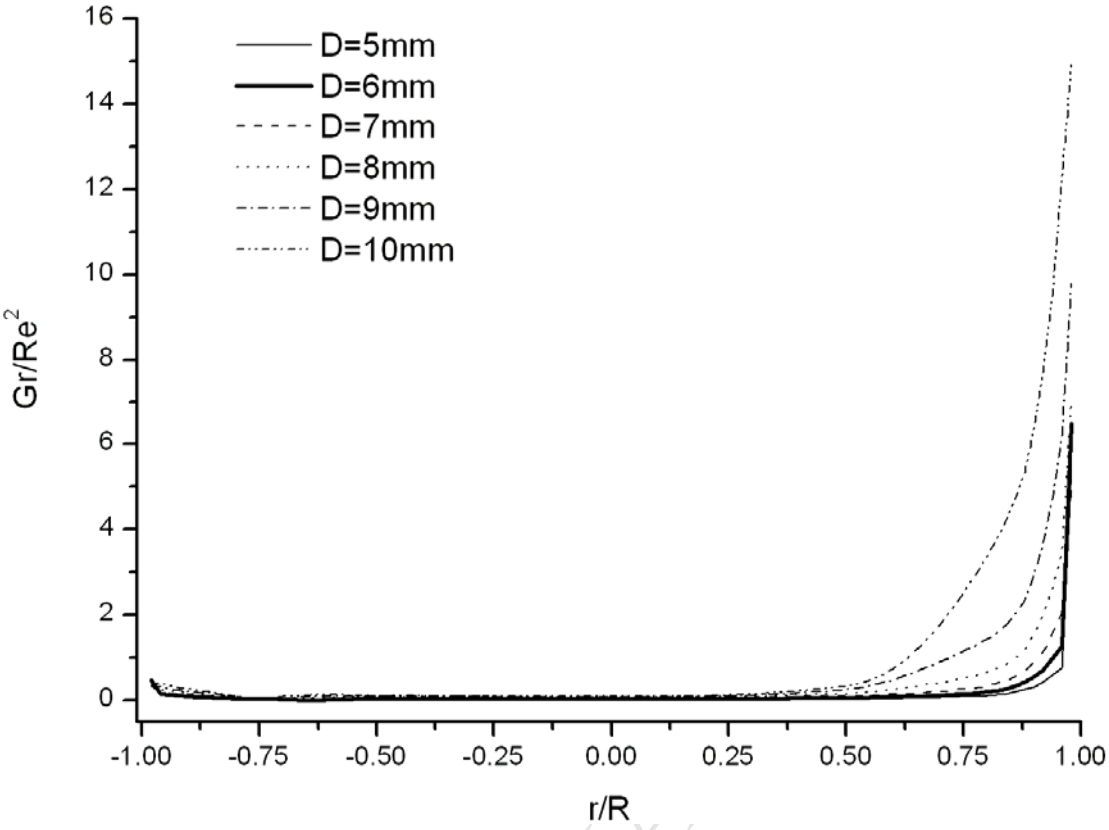

Fig. 6 Gr/Re^2 ratio comparisons at low mass flux

Title of paper: Numerical Investigation of Diameter Effect on Heat Transfer of Supercritical Water Flows in Horizontal Round Tubes

First author: Zhi Shang

The number of figures: 6

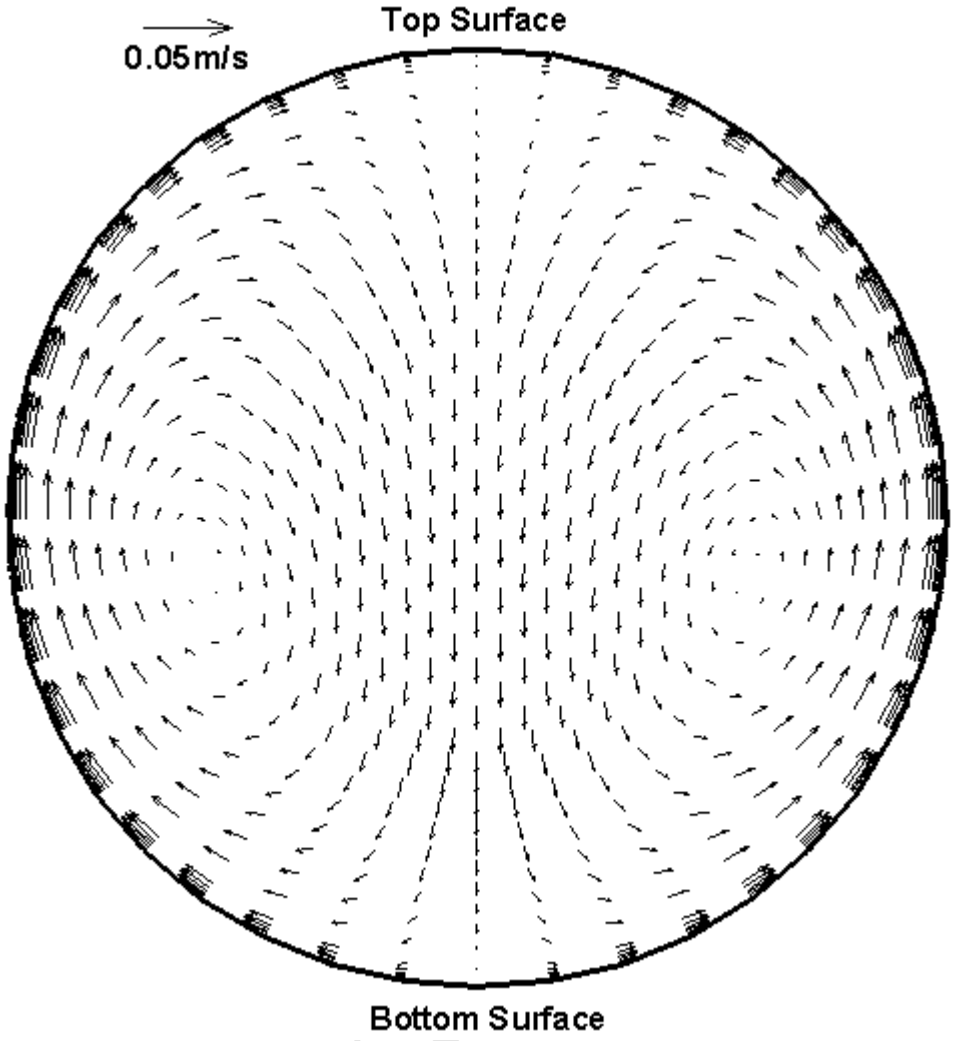

(a) D=5mm

Fig. 7 Convective flow at the cross section of the pseudo-critical point

Title of paper: Numerical Investigation of Diameter Effect on Heat Transfer of Supercritical Water Flows in Horizontal Round Tubes

First author: Zhi Shang

The number of figures: 7

The number of sub figures: (a)

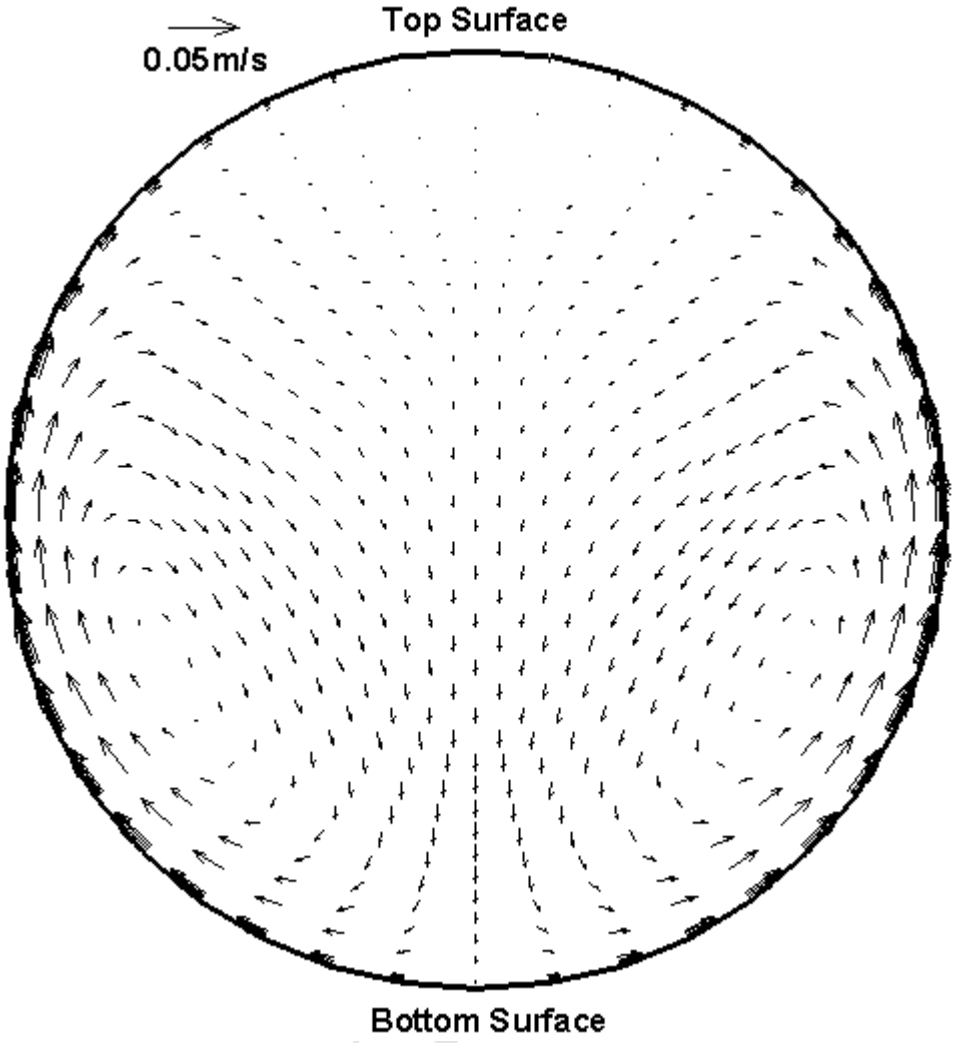

(b) D=10mm

Fig. 7 Convective flow at the cross section of the pseudo-critical point

Title of paper: Numerical Investigation of Diameter Effect on Heat Transfer of Supercritical Water Flows in Horizontal Round Tubes

First author: Zhi Shang

The number of figures: 7

The number of sub figures: (b)

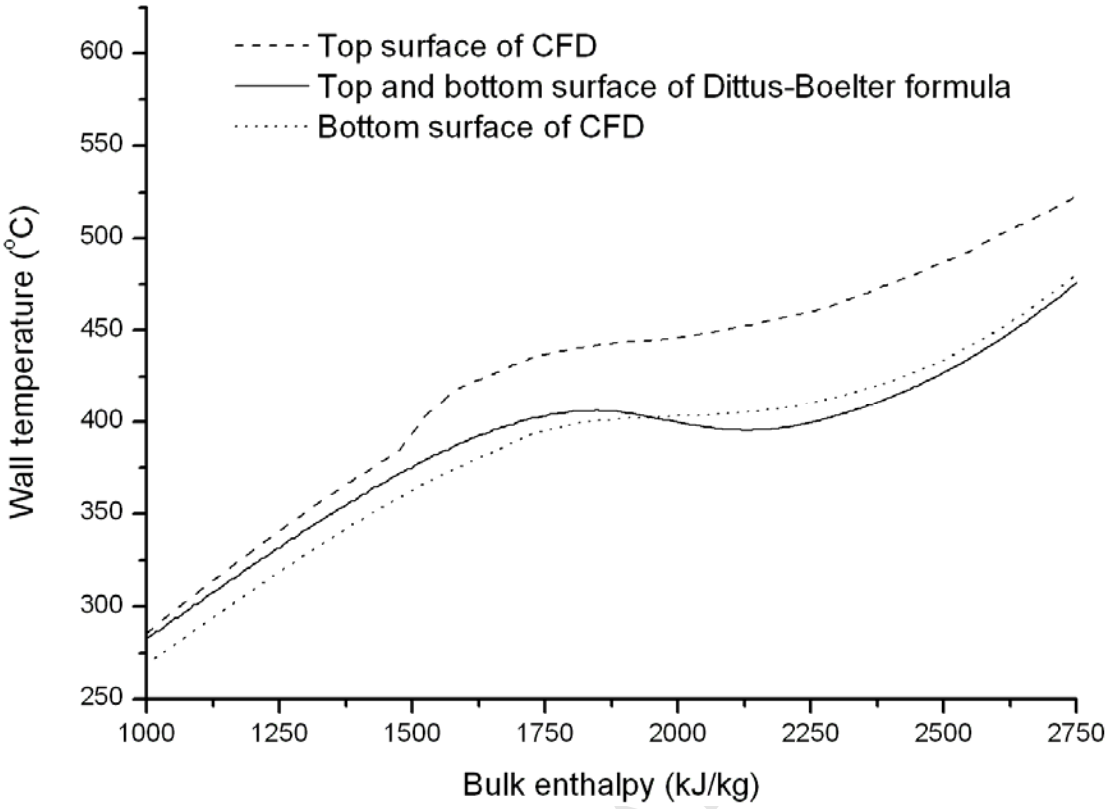

(a) D=5mm

Fig. 8 Comparisons between CFD and classical theoretical prediction

Title of paper: Numerical Investigation of Diameter Effect on Heat Transfer of Supercritical Water Flows in Horizontal Round Tubes

First author: Zhi Shang

The number of figures: 8

The number of sub figures: (a)

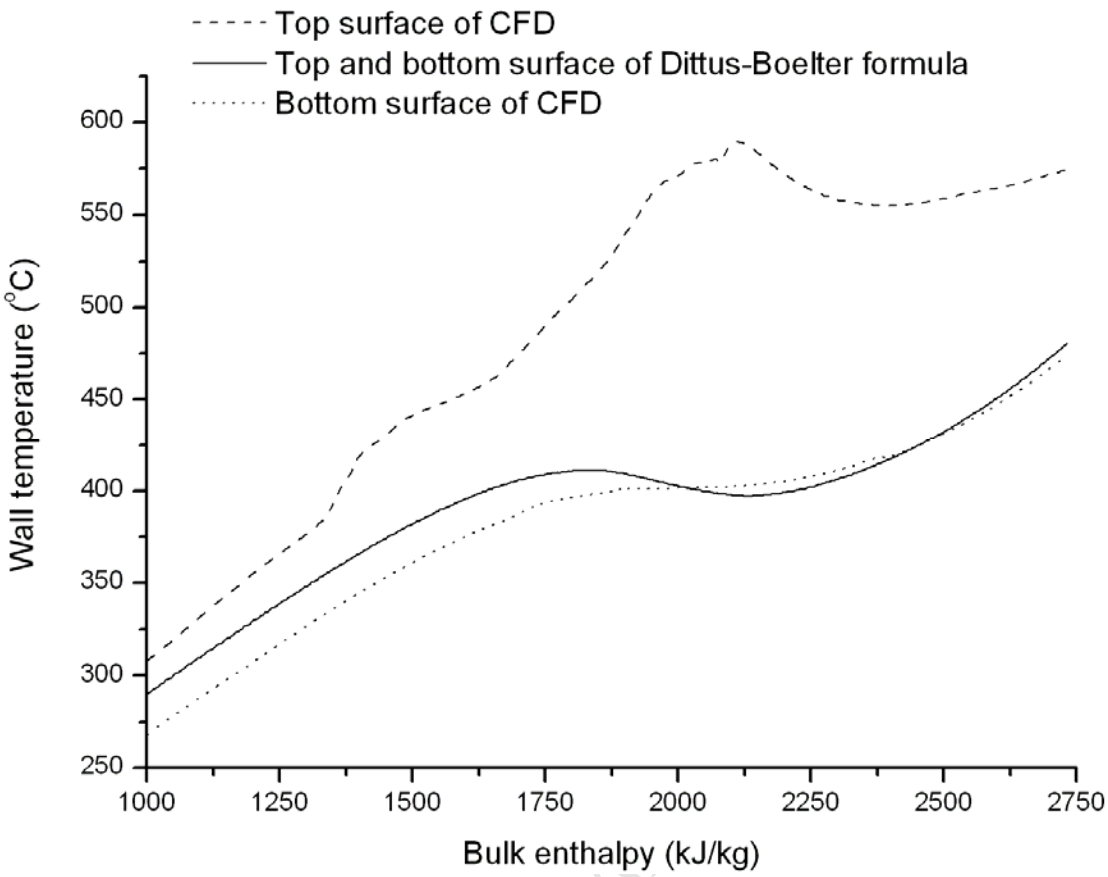

(b) D=10mm

Fig. 8 Compare between CFD and classical theoretical prediction

Title of paper: Numerical Investigation of Diameter Effect on Heat Transfer of Supercritical Water Flows in Horizontal Round Tubes

First author: Zhi Shang

The number of figures: 8

The number of sub figures: (b)

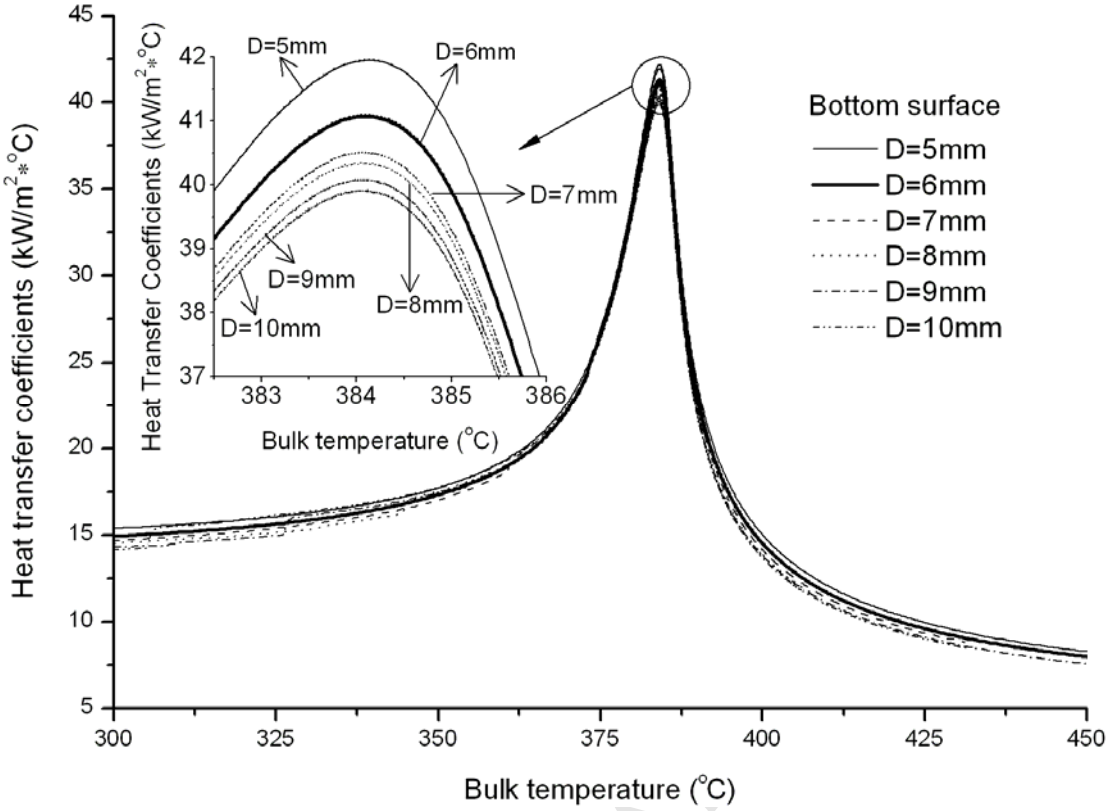

(a) At bottom surface

Fig. 9 Comparisons of different diameter influence on heat transfer coefficients

Title of paper: Numerical Investigation of Diameter Effect on Heat Transfer of Supercritical Water Flows in Horizontal Round Tubes

First author: Zhi Shang

The number of figures: 9

The number of sub figures: (a)

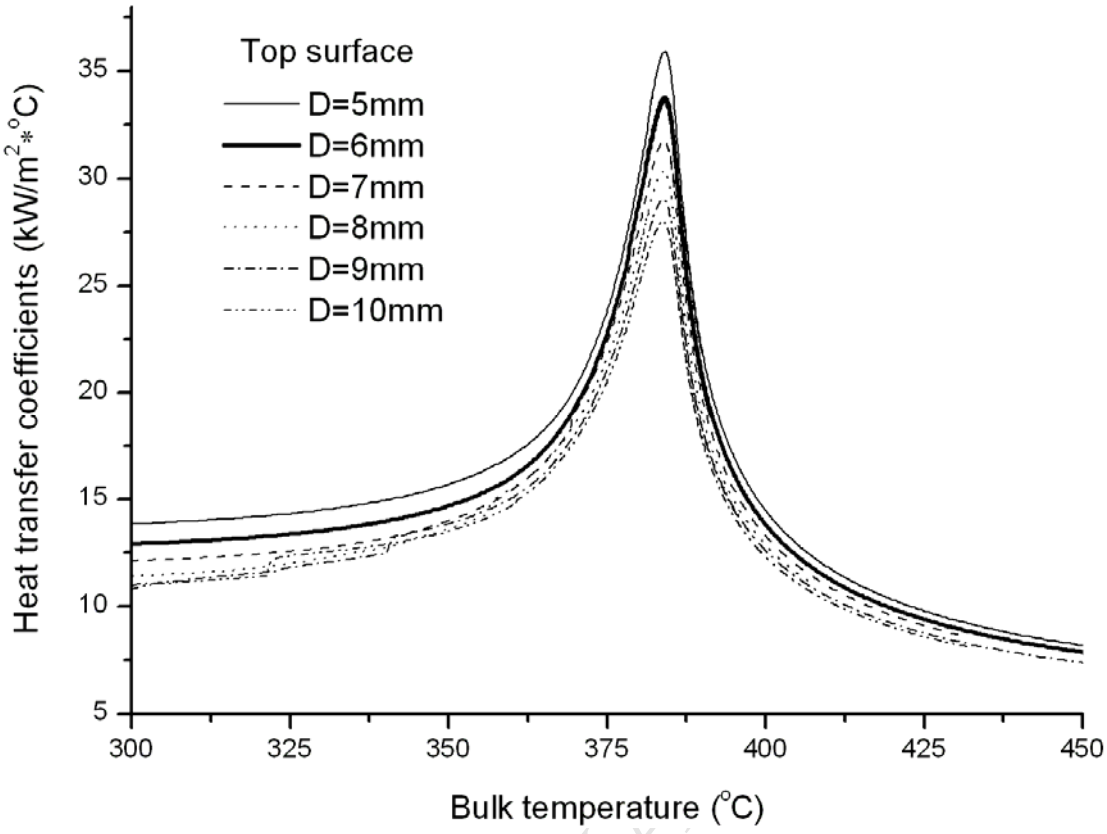

(b) At top surface

Fig. 9 Comparisons of different diameter influence on heat transfer coefficients

Title of paper: Numerical Investigation of Diameter Effect on Heat Transfer of Supercritical Water Flows in Horizontal Round Tubes

First author: Zhi Shang

The number of figures: 9

The number of sub figures: (b)

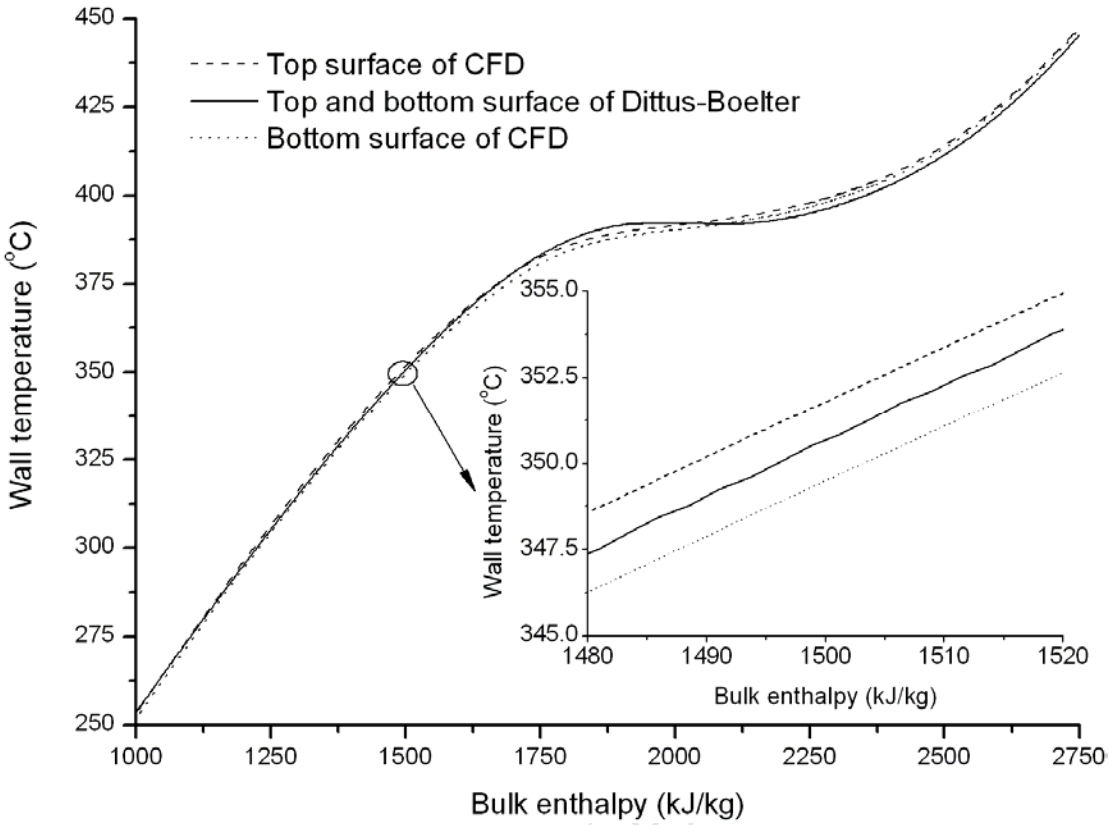

(a) D=5mm

Fig. 10 Comparisons between CFD and Dittus-Boelter formula

Title of paper: Numerical Investigation of Diameter Effect on Heat Transfer of Supercritical Water Flows in Horizontal Round Tubes

First author: Zhi Shang

The number of figures: 10

The number of sub figures: (a)

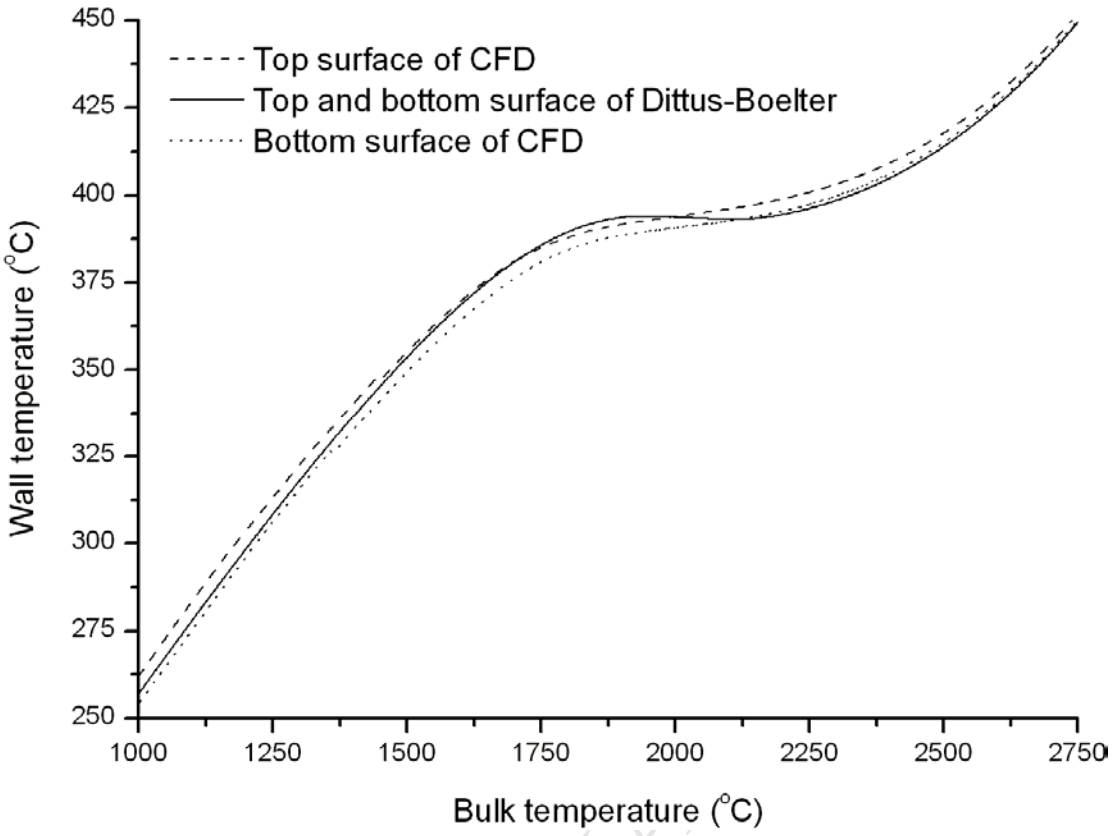

(b) D=10mm

Fig. 10 Comparisons between CFD and Dittus-Boelter formula

Title of paper: Numerical Investigation of Diameter Effect on Heat Transfer of Supercritical Water Flows in Horizontal Round Tubes

First author: Zhi Shang

The number of figures: 10

The number of sub figures: (b)

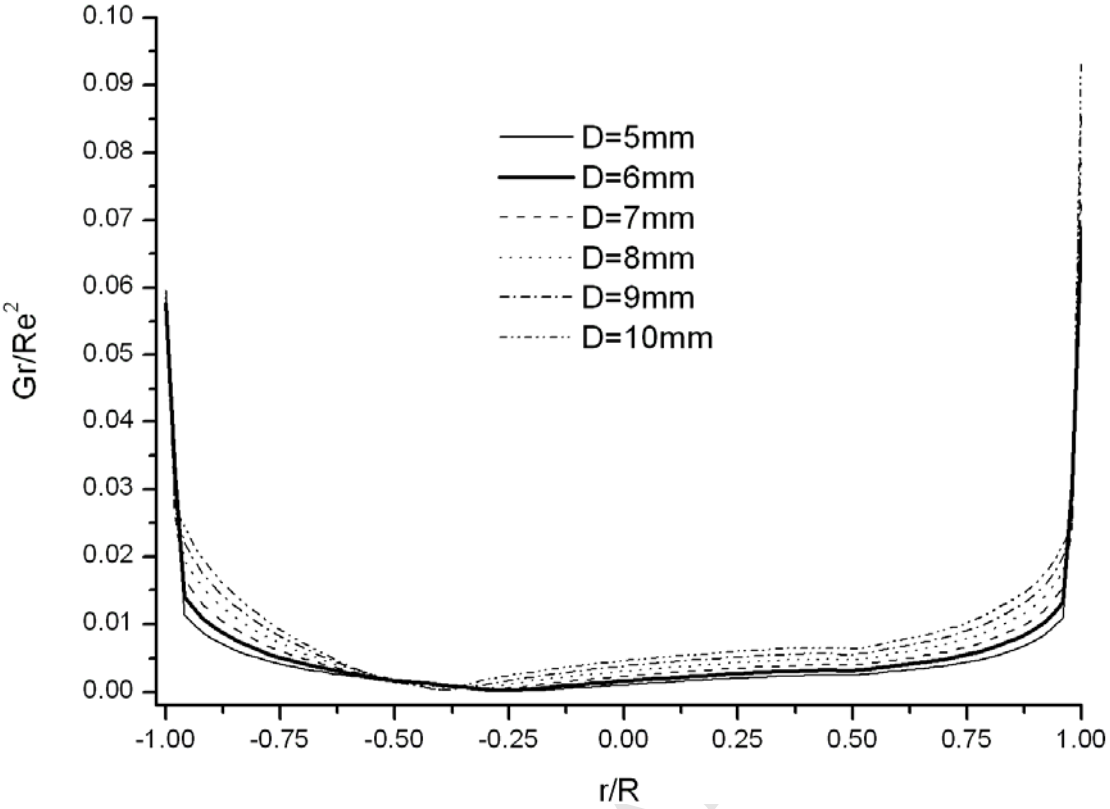

Fig. 11 Gr/Re^2 ratio comparisons at high mass flux

Title of paper: Numerical Investigation of Diameter Effect on Heat Transfer of Supercritical Water Flows in Horizontal Round Tubes

First author: Zhi Shang

The number of figures: 11

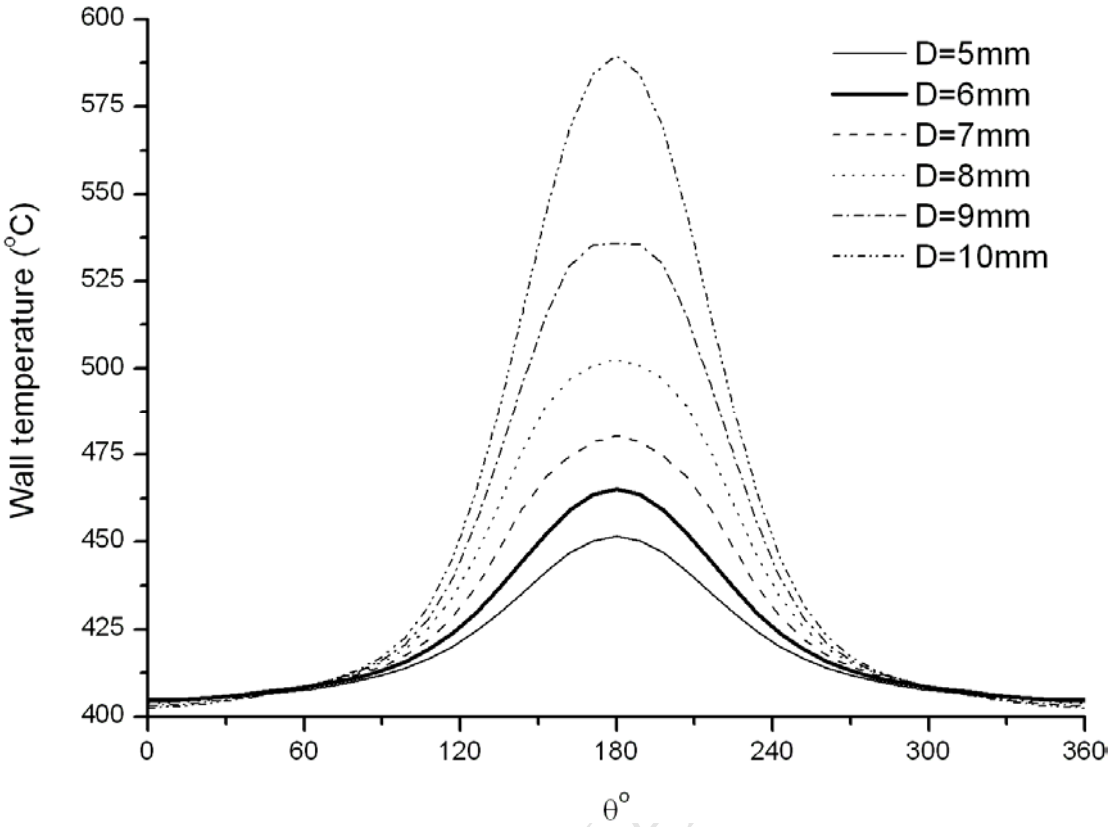

(a) Low mass flux

Fig. 12 Wall temperature distributions along circumference

Title of paper: Numerical Investigation of Diameter Effect on Heat Transfer of Supercritical Water Flows in Horizontal Round Tubes

First author: Zhi Shang

The number of figures: 12

The number of sub figures: (a)

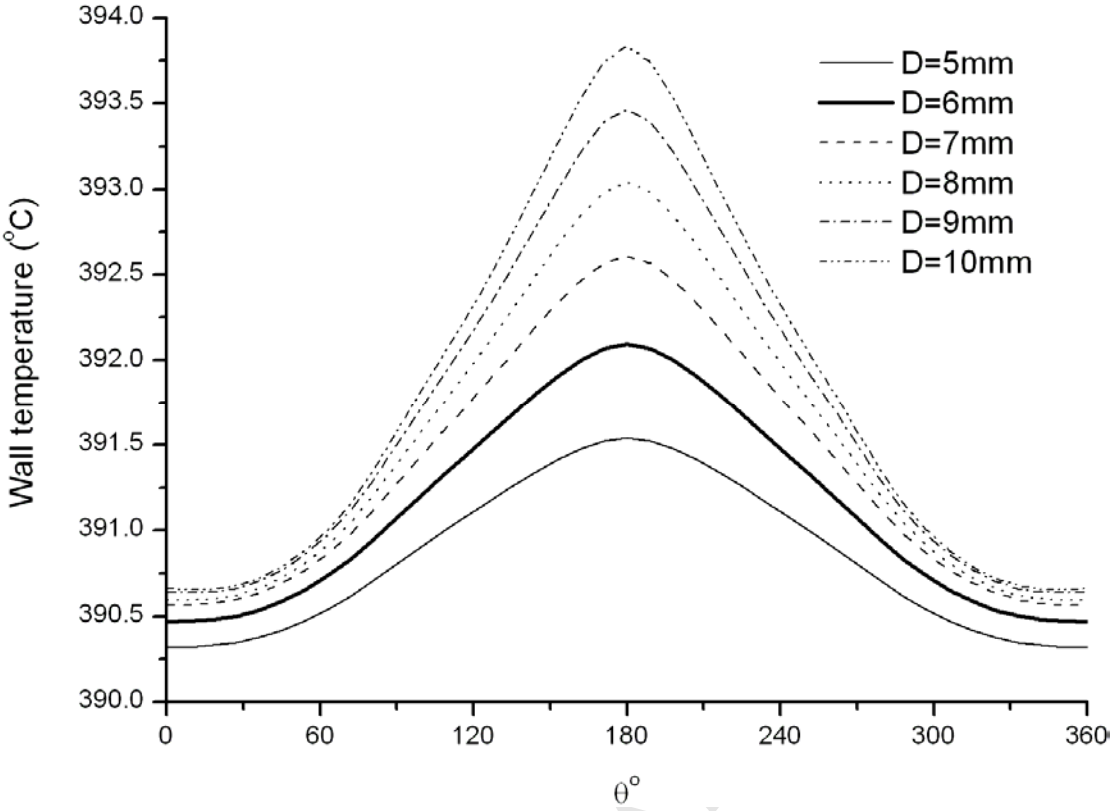

(b) High mass flux

Fig. 12 Wall temperature distributions along circumference

Title of paper: Numerical Investigation of Diameter Effect on Heat Transfer of Supercritical Water Flows in Horizontal Round Tubes

First author: Zhi Shang

The number of figures: 12

The number of sub figures: (b)

Table 1 Coefficients of the Speziale non-linear high Reynolds k-ε turbulence model

C_μ	σ_k	σ_ε	σ_h	$C_{\varepsilon 1}$	$C_{\varepsilon 2}$	$C_{\varepsilon 3}$	$C_{\varepsilon 4}$
0.09	1.0	1.219	0.9	1.44	1.92	1.44	-0.33

Title of paper: Numerical Investigation of Diameter Effect on Heat Transfer of Supercritical Water Flows in Horizontal Round Tubes

First author: Zhi Shang

The number of tables: 1

Table 2 Convective differencing discretization schemes

Cases	Discretization scheme	Accuracy of differencing scheme
1	CD	second order
2	LUD	second order
3	MARS	second order
4	QUICK	third order

Title of paper: Numerical Investigation of Diameter Effect on Heat Transfer of Supercritical Water Flows in Horizontal Round Tubes

First author: Zhi Shang

The number of tables: 2

Table 3 Flow conditions of simulation cases

Cases	System pressure	Mass flux	Heat flux	Diameters
5 – 10	24.4 MPa	340 kg/m^{2}s	300 kW/m^2	5 – 10 mm
11 –16	24.4 MPa	964 kg/m^{2}s	307 kW/m^2	5 – 10 mm

Title of paper: Numerical Investigation of Diameter Effect on Heat Transfer of Supercritical Water Flows in Horizontal Round Tubes

First author: Zhi Shang

The number of tables: 3